

Erosion, Contamination, and Migration

Jim Strachan, PPPL

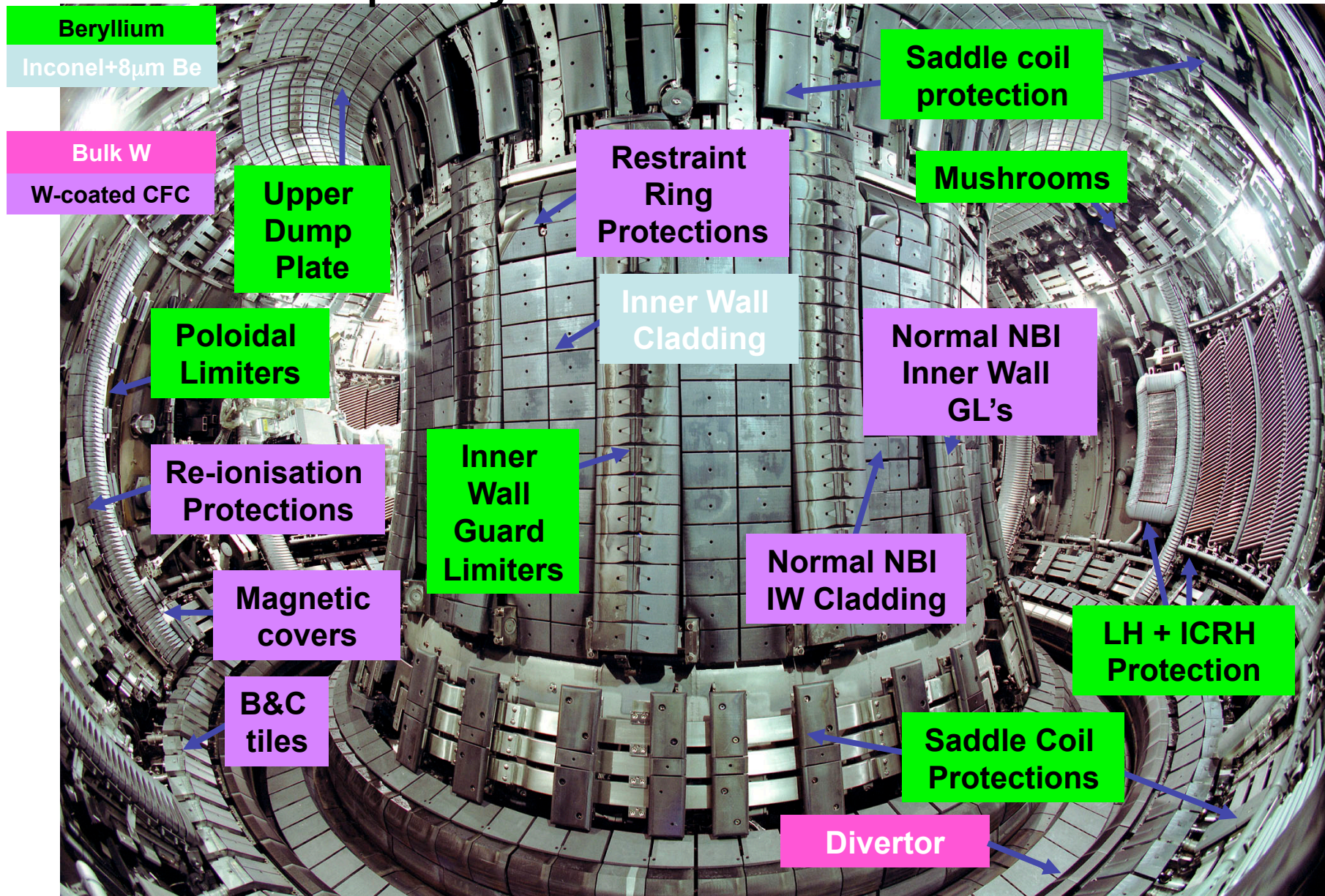
IIS09, June, 2009,

- **Perspective:**
 - **Use the JET methane gas injection experiments to understand JET carbon impurity source, contamination, and migration. Then use these studies to relate to ITER**
- **Outline:**
 - **1. JET carbon sources**
 - **2. JET carbon contamination**
 - **3. JET carbon migration**
 - **4. Relate to ITER**

Impurity sources

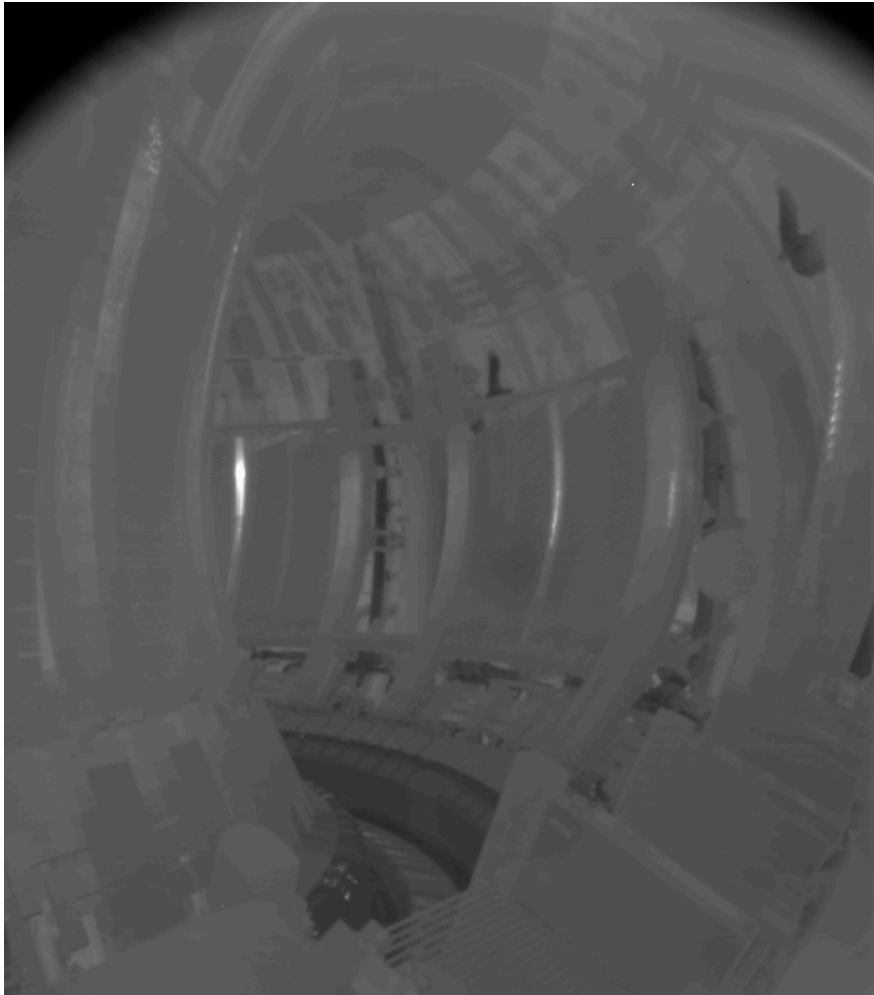
- Status of existing tokamak studies: still uncertainty about which sources dominate the contamination
- Generally expect:
 - Wall sources
 - Core neutral CX bombardment
 - SOL ion bombardment
 - ELMs, filaments, and disruption events
 - RF accelerated ions
 - Divertor sources
 - Ion bombardment along the targets is dominant
- Release rates in JET seem factor-of-two in agreement with chemical sputtering rates

Impurity Influx from 3D Sources

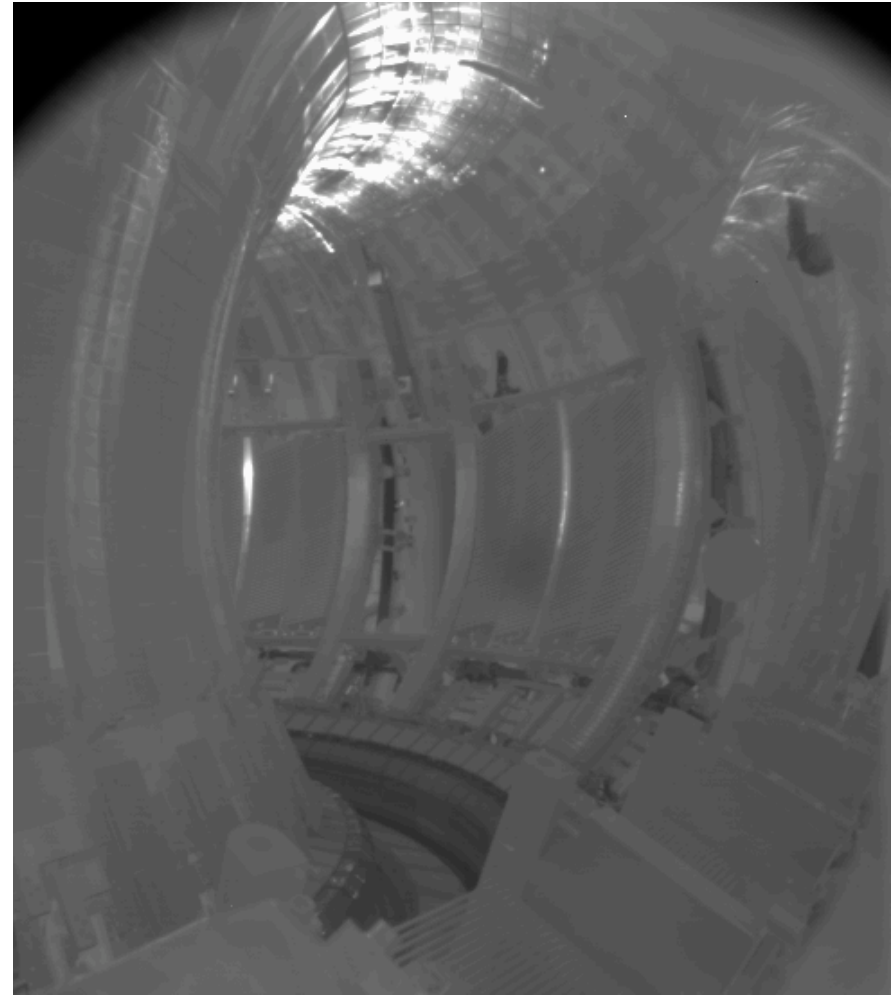


Infra-Red Images indicate plasma contact

Quiescent plasma

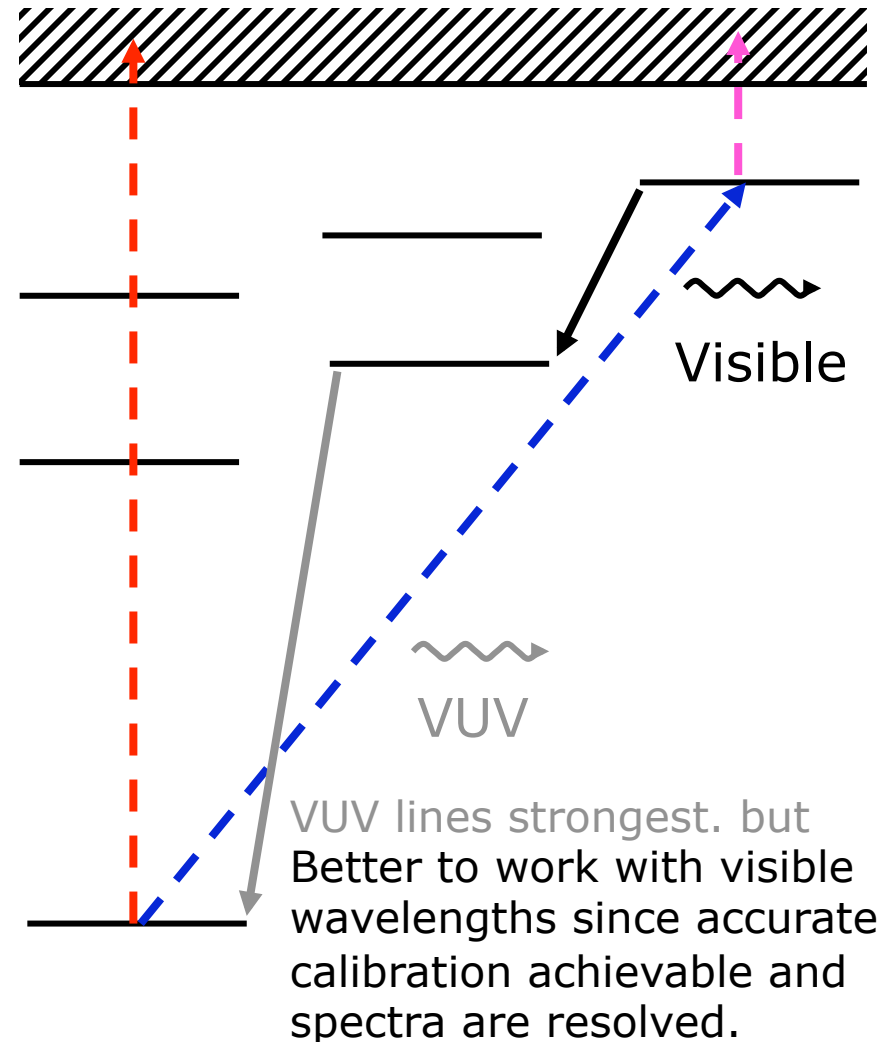


Small disruption Disruption

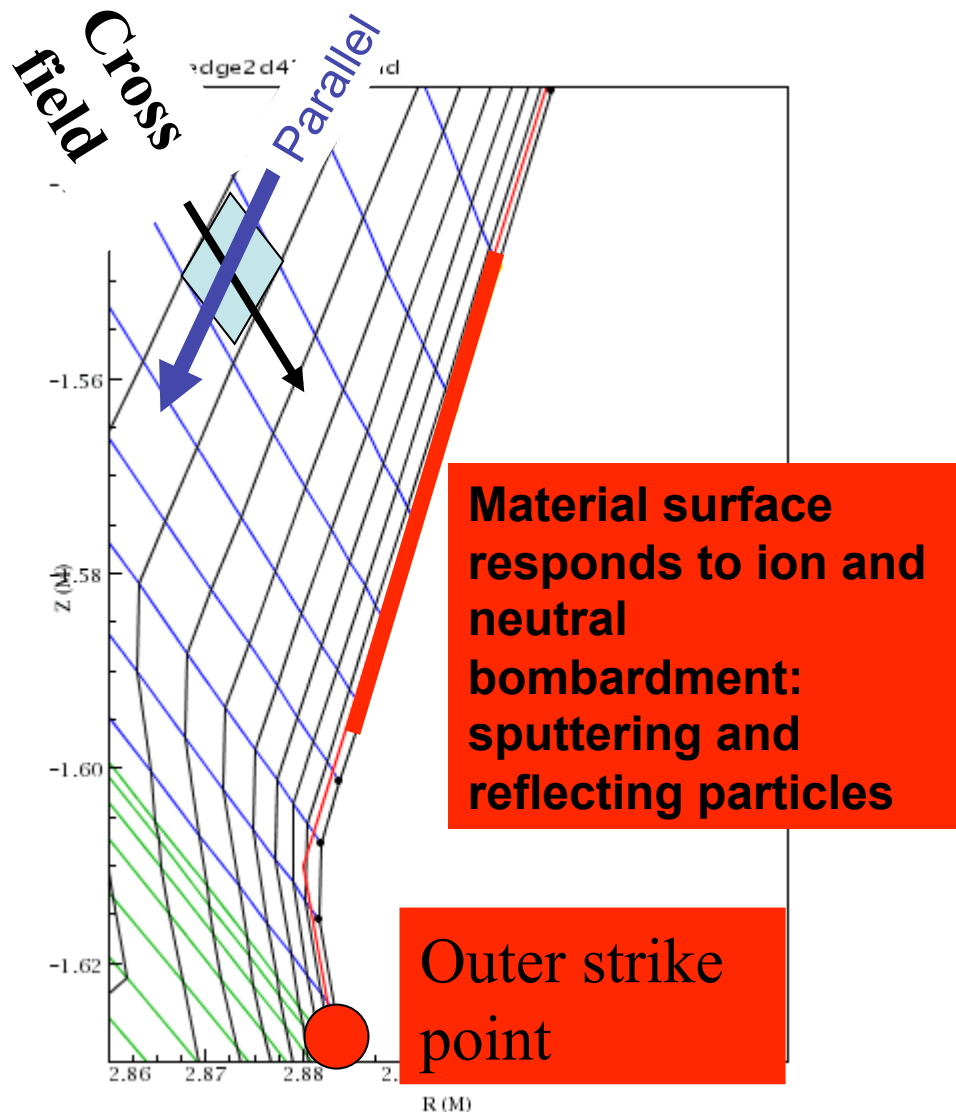


Atomic physics basis for erosion measurement

- Atoms or ions entering a hot plasma will either get **ionised** (which we cannot see) or become **excited** and emit a photon (which we can see).
- Ratio of “**Ionisations per Photon**” is used to turn measured intensity (**ph/sec**) into erosion rate (**ions/sec**).
- With increased temperature, the rate coefficient for ionisation increases more strongly than excitation.
- With increased density, **step-wise ionisation** can play a role.



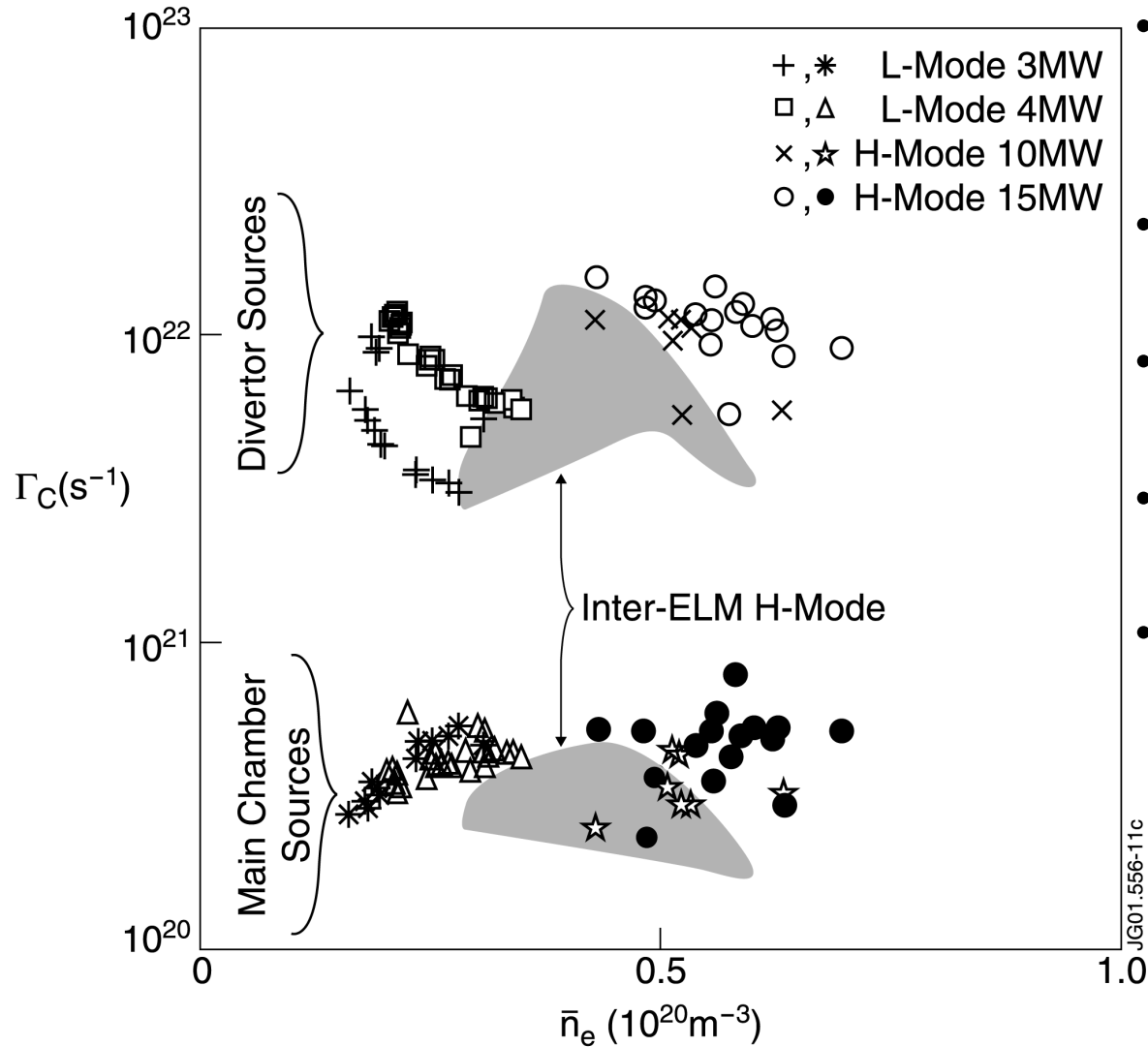
EDGE2D/NIMBUS calculates fluid motion of SOL plasma



EDGE2D calculates 2 dimensional electrons, deuterium ions, and each carbon charge state in the cells of the grid connecting each by either parallel or perpendicular transport.

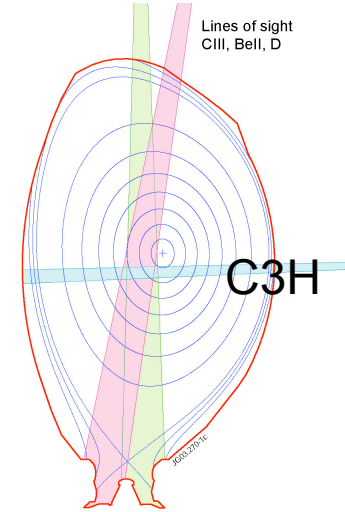
NIMBUS calculates Monte Carlo deuterium molecules, and atoms, as well as carbon atoms, on a mesh which fills the machine volume

CIII light indicates intrinsic C Influx



- Impurity content result of 3 processes: sources, screening, and confinement
- DIVIMP related CIII light to Γ_C
- Divertor sources larger than wall sources
- divertor sources increase with applied power
- L-Mode: wall sources increase and divertor sources decrease with density

C3H provides a good approximation to the carbon ionization in the SOL



Experimentally, the Yield is defined by the ratio of carbon to deuterium Light. EDGE2D, indicates that this ratio correlates with the Carbon to deuterium ionization rates in the SOL

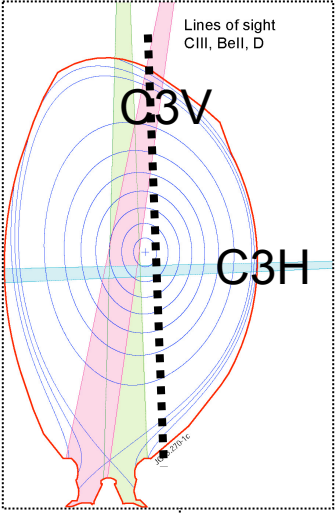




SOL ionization rates: D rate is similar for EDGE2D, JET L-Mode, and JET Inter-ELM H-Mode, with experiment extending to higher values. C rate is similar for EDGE2D and L-Mode but higher for H-Mode

Compare to Experiment:

JET L-MODE plasmas have CIII signals like a uniform wall source



unity

Outline

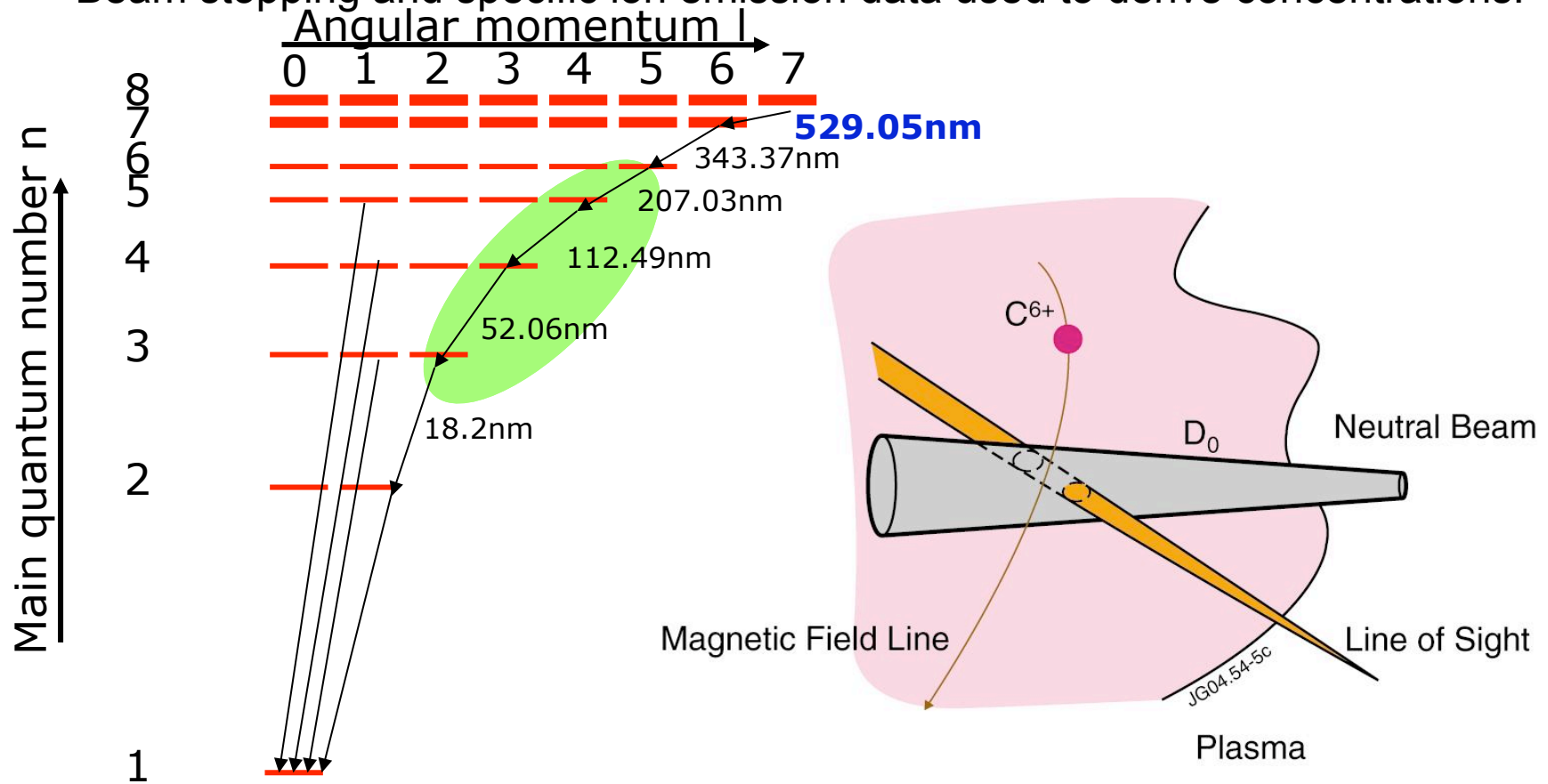
- 1. **JET carbon sources**
 - **C/D light can measure sputtering rate**
 - **Narrow selection of discharges to infer sputtering**
 - **Chemical sputtering of carbon is important**
 - **Factor-of-two agreement with published sputtering coefficients**
 - **ELM is major difference between L & H Mode but other differences do exist**
- 2. *JET carbon contamination*
- 3. *JET carbon migration*
- 4. *Relate to ITER*

Contamination

- We reached some level of understanding about the JET carbon contamination during quiescent plasma, which are not
 - too close to the walls,
 - High triangularity (close to the top) and
 - with ICRF
- Understanding probably does not extend to ITER due to unknown physics origin of SOL flows, ITER interaction at vessel top, and W/Be (not C) composition of ITER components

C⁺⁶ measurement by CX spectroscopy

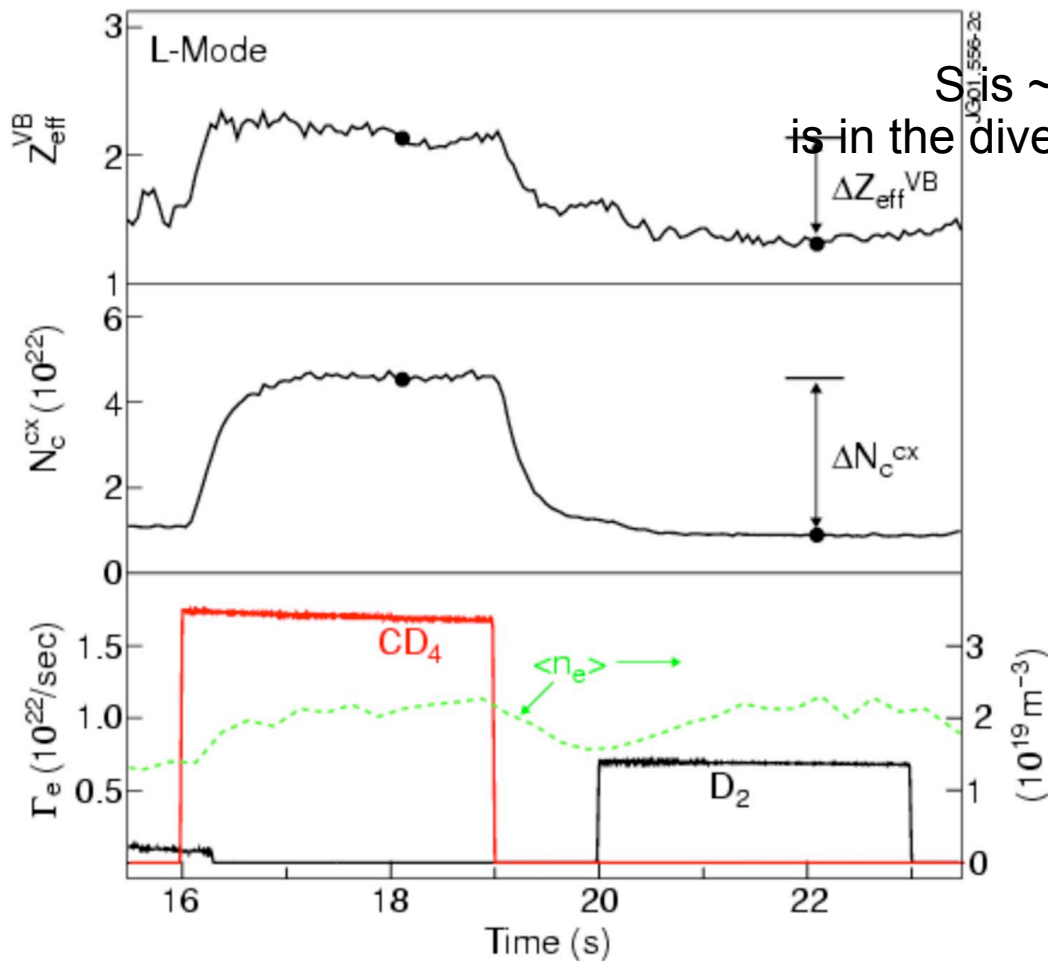
- Charge exchange process populate predominantly $n=Z^{3/4}$
- Use **visible wavelengths** for accurate absolute calibration, high spectral dispersion and good imaging to achieve local measurement.
- Beam stopping and specific ion emission data used to derive concentrations.



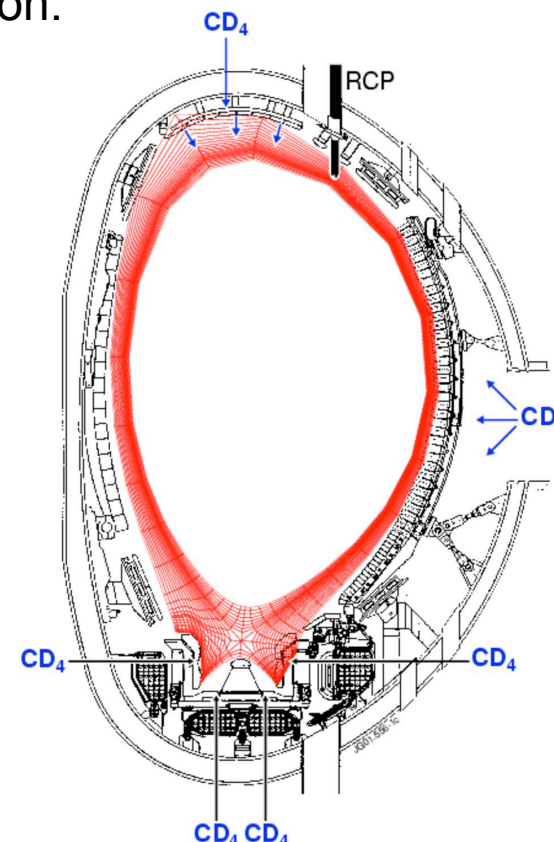
CD₄ puff experiments: Impurity screening

$S = \Delta N_c / \Gamma_c \tau^*$: Screening number – Fraction actually entering confined plasma

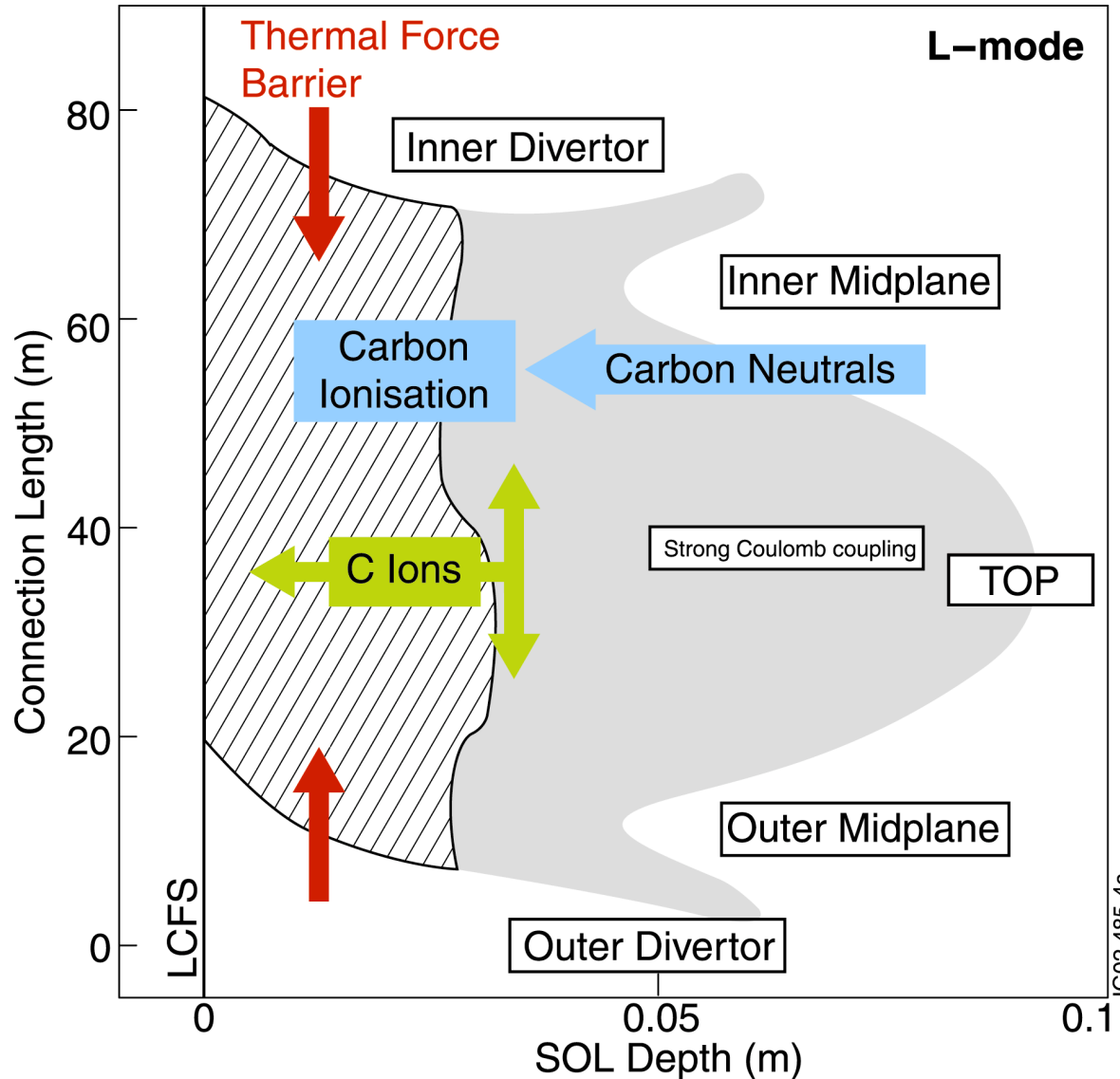
τ^* : Rate of rise of Carbon content Γ_c : Carbon influx applied during experiment



S is ~ 5-10 times lower if injection is in the divertor region.



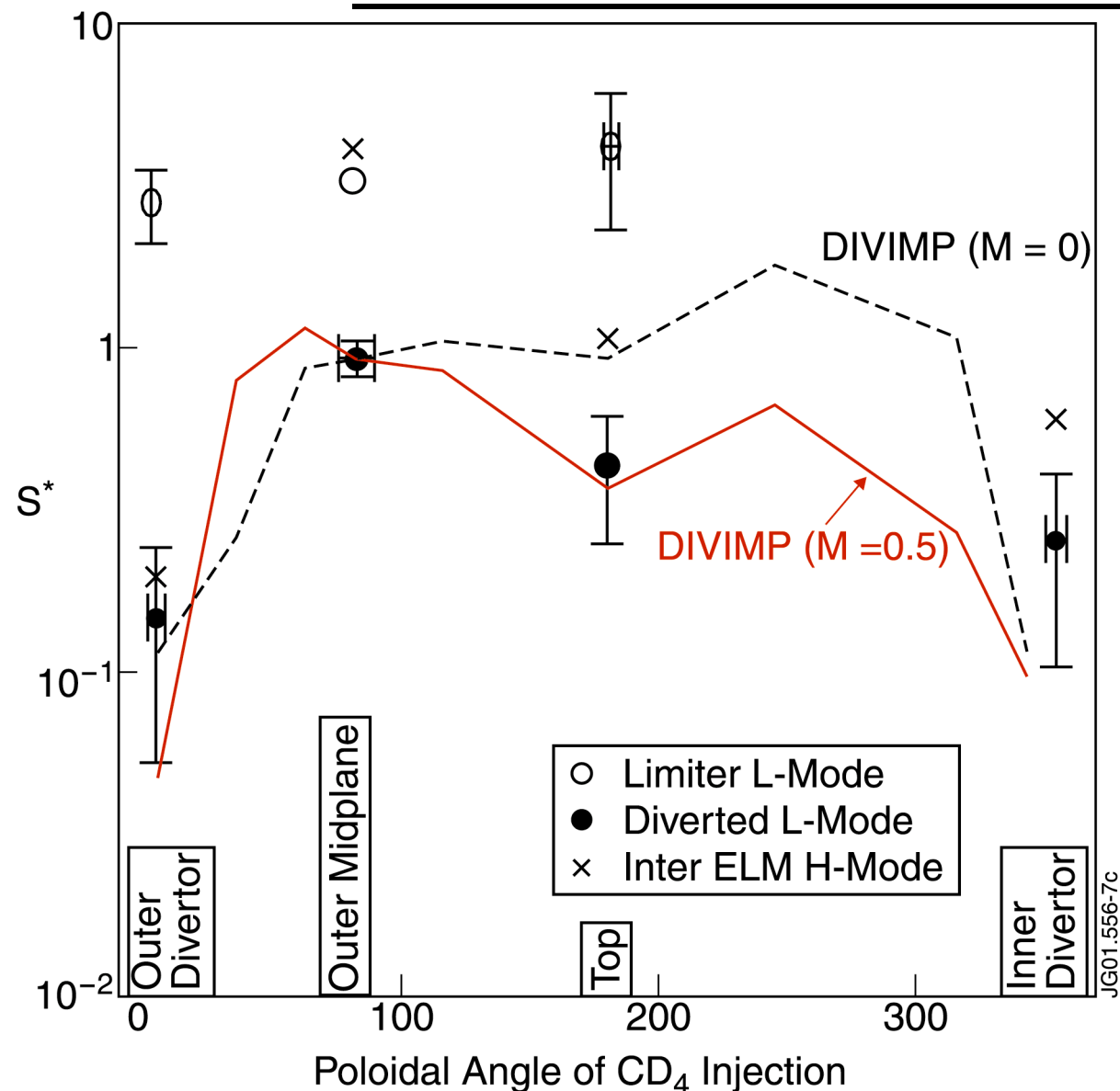
Main Chamber Carbon Processes



- Diffusion wins near LCFS
- Parallel transport wins at lower temps
- C ionisation in Diffusion region
- Thermal Force blocks C escape

JG02.485-4c

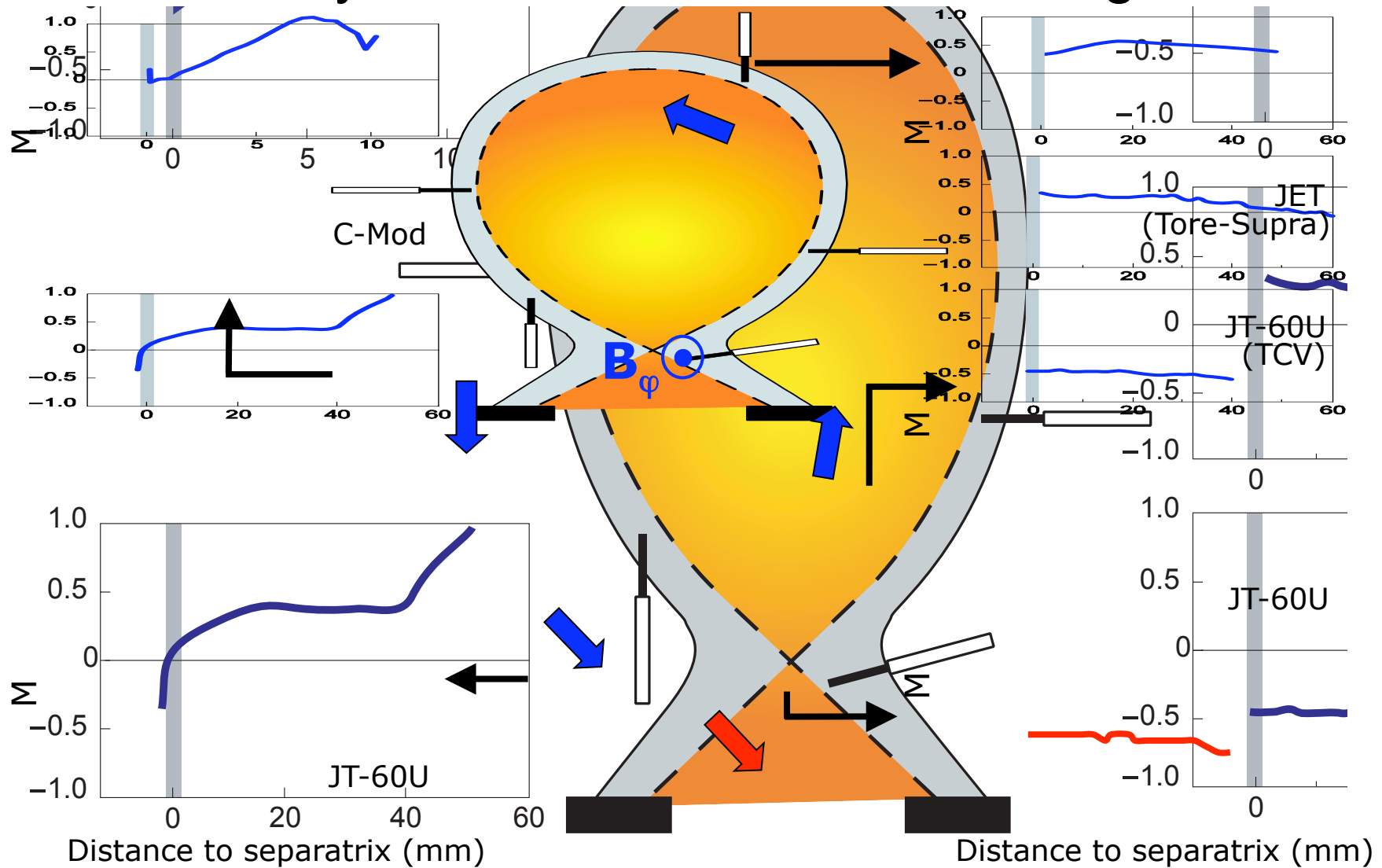
Divertor vs Limiter Screening



- $DIVIMP$ normalised to mid-plane screening (adjusting Carbon D)
- SOL flow influenced top screening
- Inter-ELM H-Mode screening worse than L-Mode, but similar location dependence

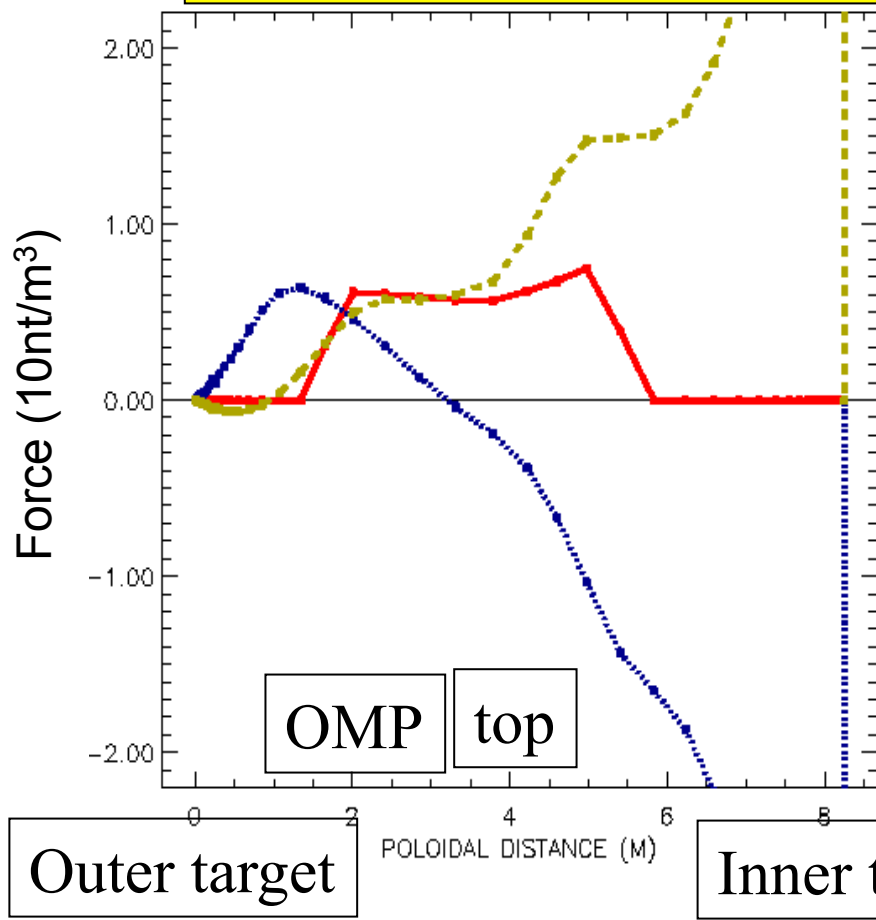
JG01.556-7c

Deuterium SOL flow: parallel Mach Number, $M = v_{\parallel}/c_s$.
 Mostly **POSITIVE** towards inner target

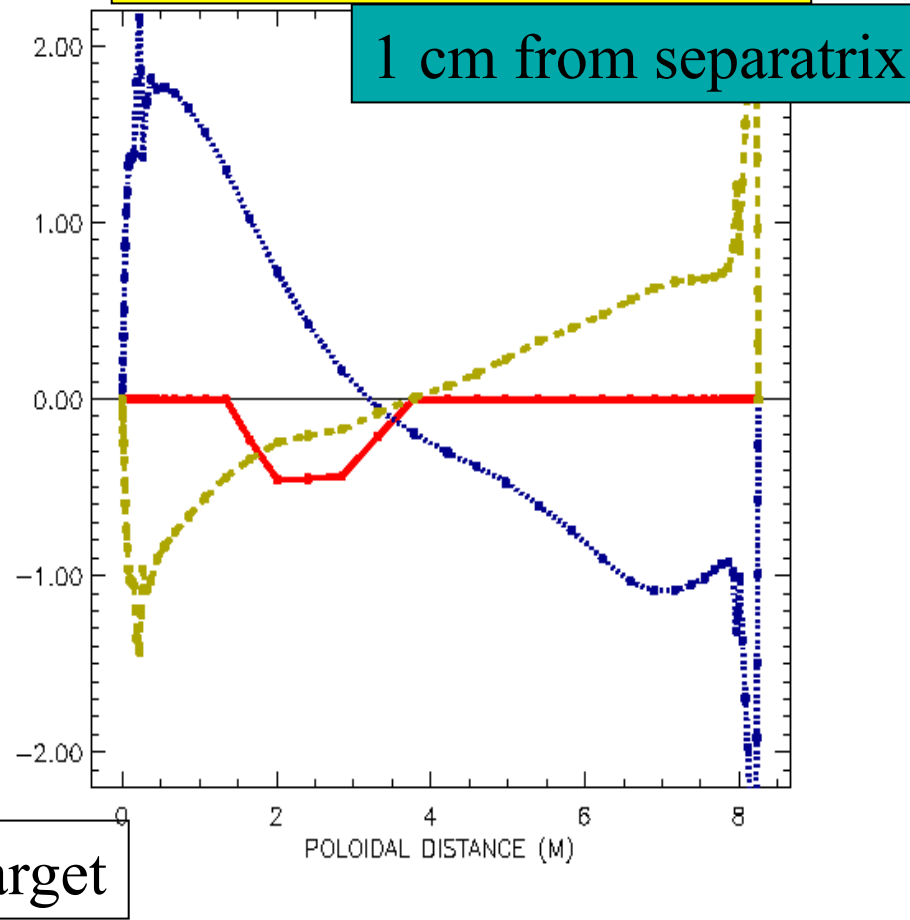


Magnitude of the applied force is significant, but not dominant. Used a force applied to large major radius, and 2 cm into SOL from separatrix

Flows similar to normal fields

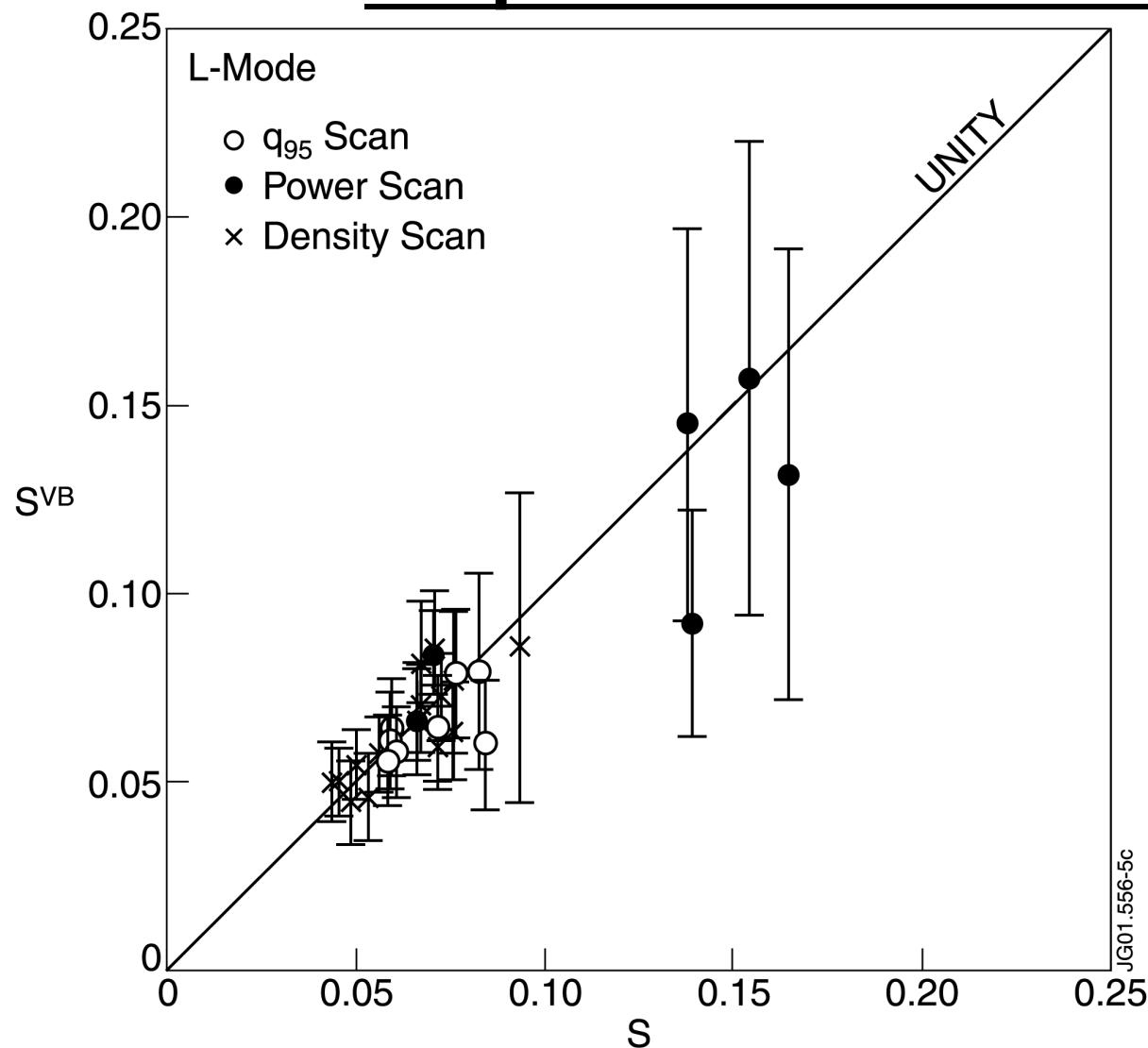


Flows similar to reverse field



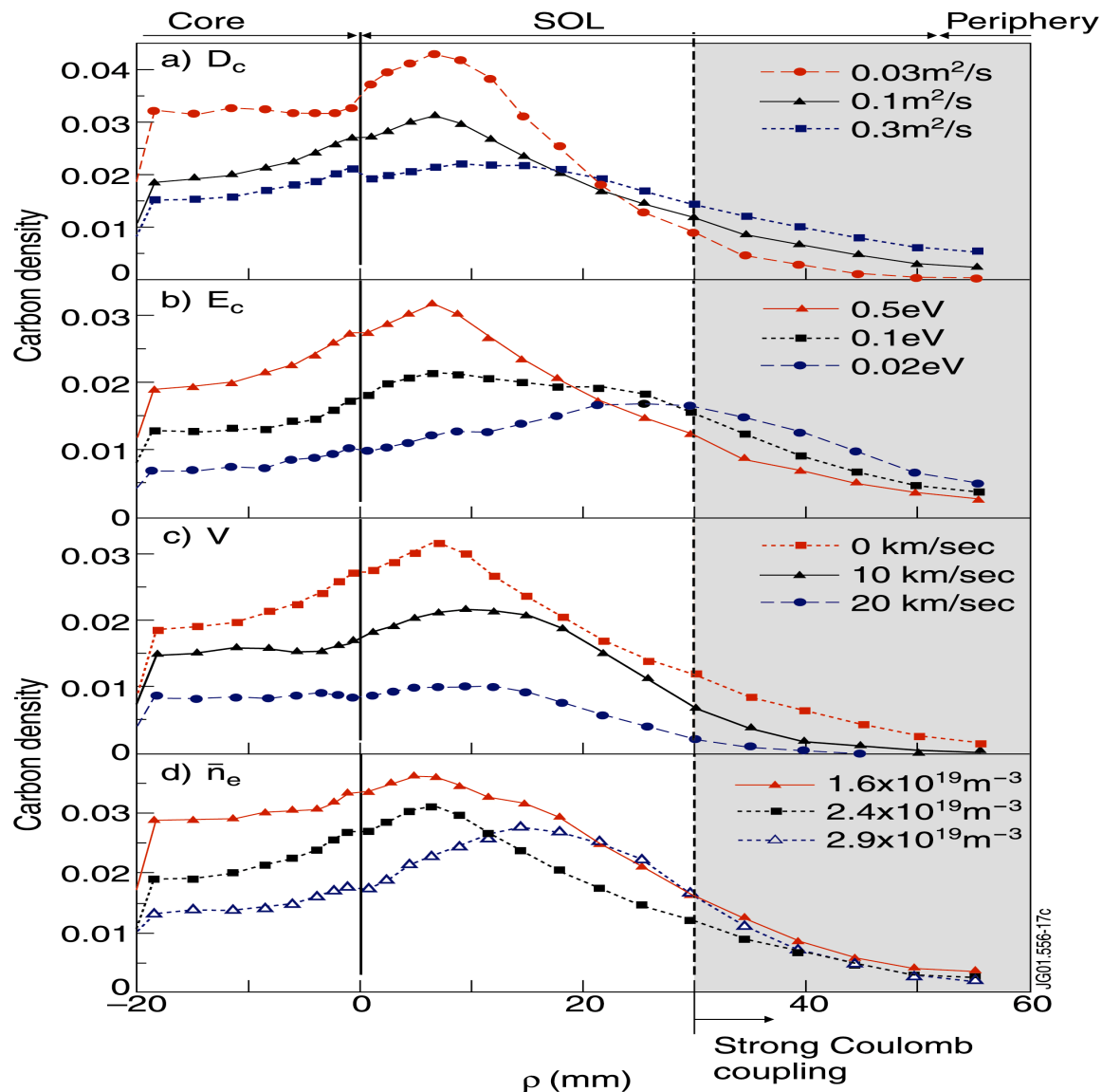
Red=external force, blue=thermal force, green=friction force

Empirical L-Mode Screening



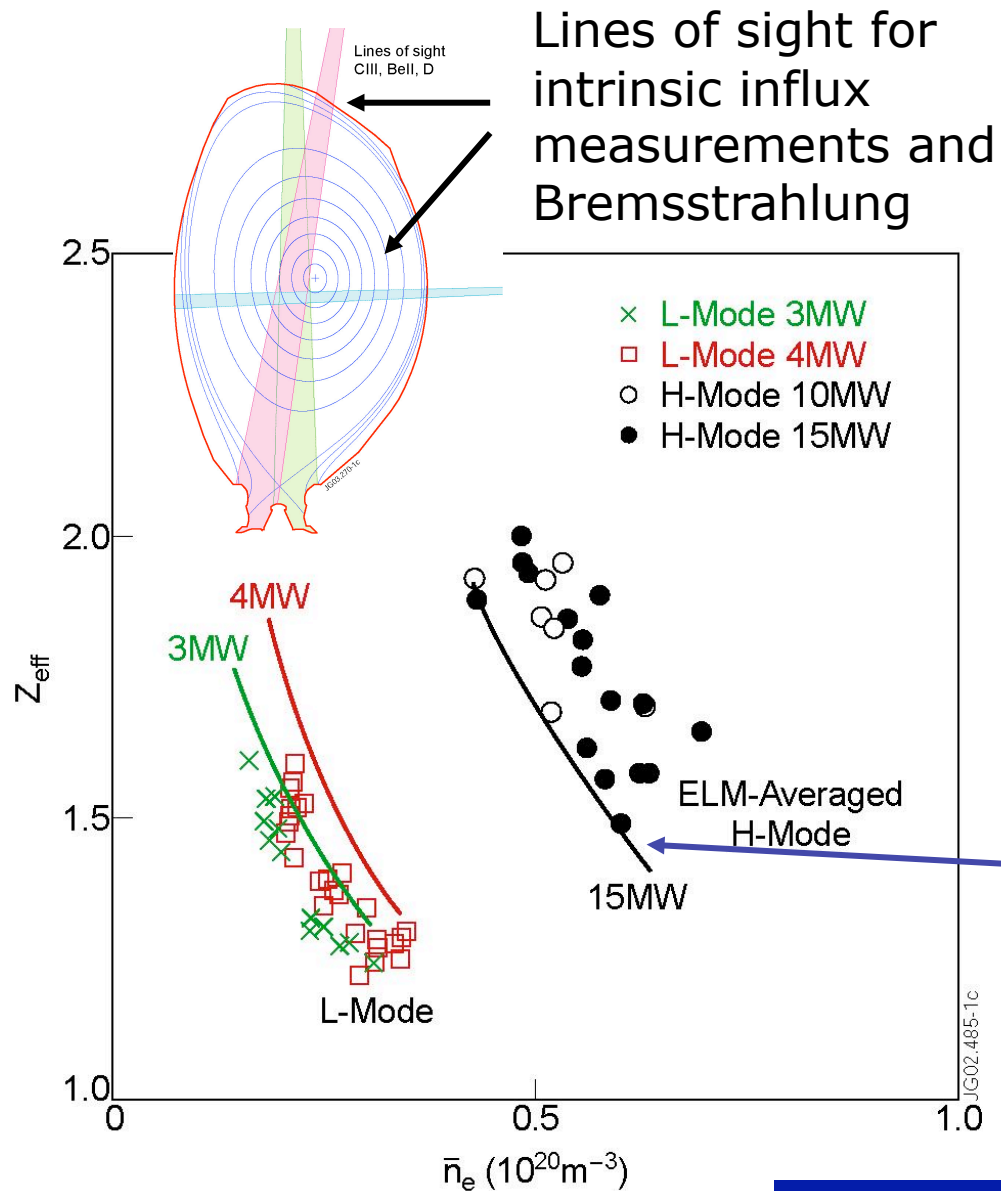
- mid-plane CD_4 injection
- varied parameters important for intrinsic Z_{eff} and/or SOL
- $S \propto 1/n_e \tau_E$
- or: $S \propto Pq^{1/2}/n_e$

DIVIMP Screening trends



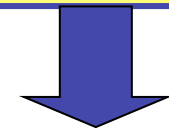
- Higher C diff. Increases access to region of high coupling
- high flows increase connection to divertor
- higher density or lower initial C energy increases the distance from ionisation to LCFS

Carbon source consistent with Carbon dominated Z_{eff}



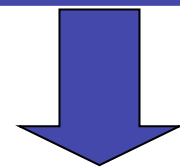
Intrinsic C-source

Divertor source =
5-10 x Wall source



Empirical screening

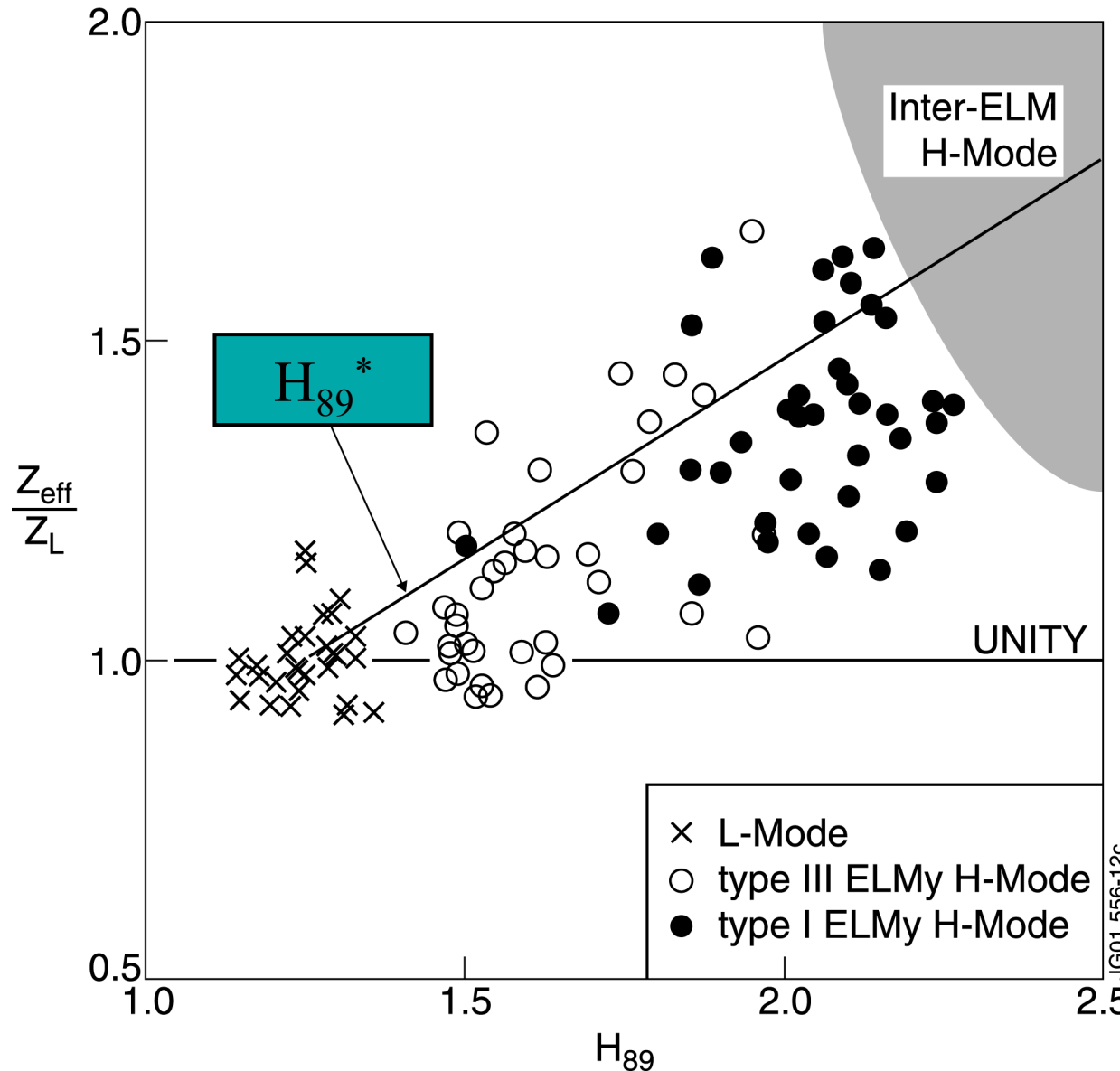
Divertor screening =
5-10 x Wall screening



Predict intrinsic Z_{eff}

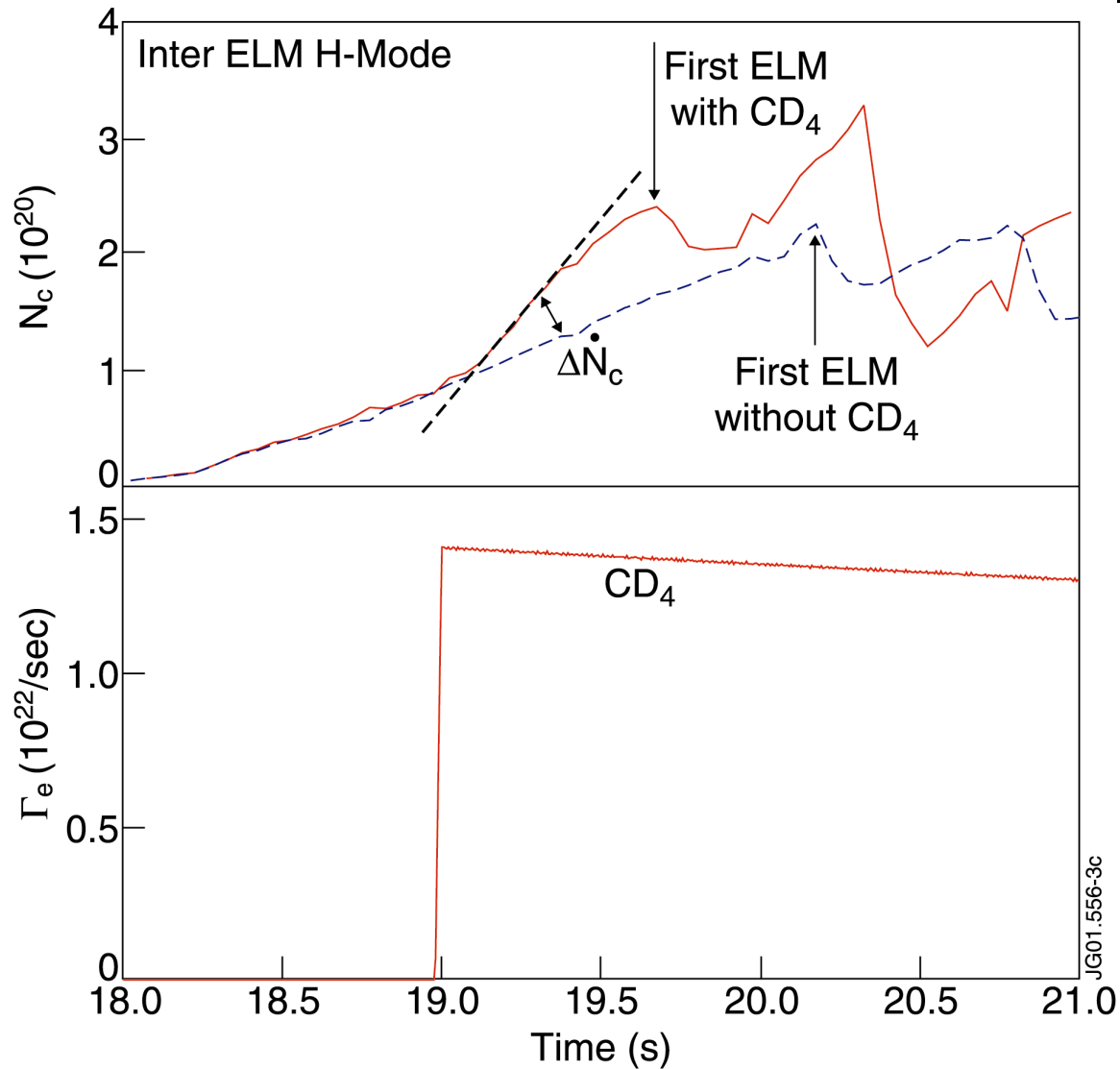
$$1 + \sum Z(Z-1)n_Z \sim 1 + 30n_C$$

Intrinsic Z_{eff} Trends



- L-Mode:
 $Z_{\text{eff}} = Z_L \propto P^{.2}/n^{.3}$
- H-Mode:
 $Z_{\text{eff}} = Z_L H_{89}^{.9}$
- Impurity confinement probably different between L- and H-Modes
- ELM effects incorporated into H_{89}

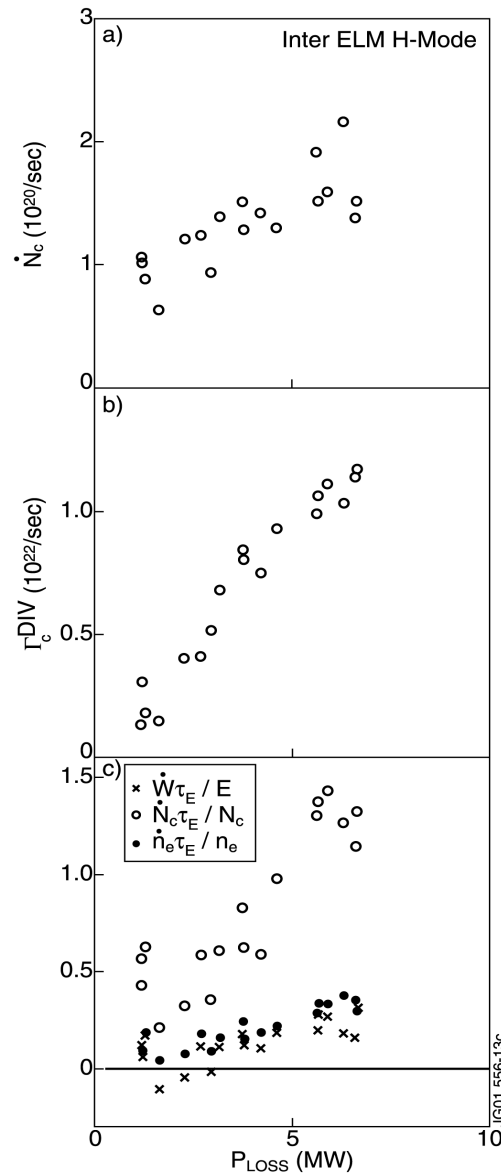
Inter ELM H-Mode



- In the limit $t \ll \tau_p$:

$$S = \Delta(dN_c/dt)/\Gamma_c$$
- Core CX had less statistical noise and required to measure derivative
- CD_4 and D_2 injection could induce the first ELM

Divertor C source dominates Inter ELM Z_{eff}



- Carbon content rate of rise and divertor carbon influx prop to power flow into divertor
- more C originates from divertor than L-Mode
- Long period ELM plasmas - higher power required higher current
- C accumulation dominates these plasmas

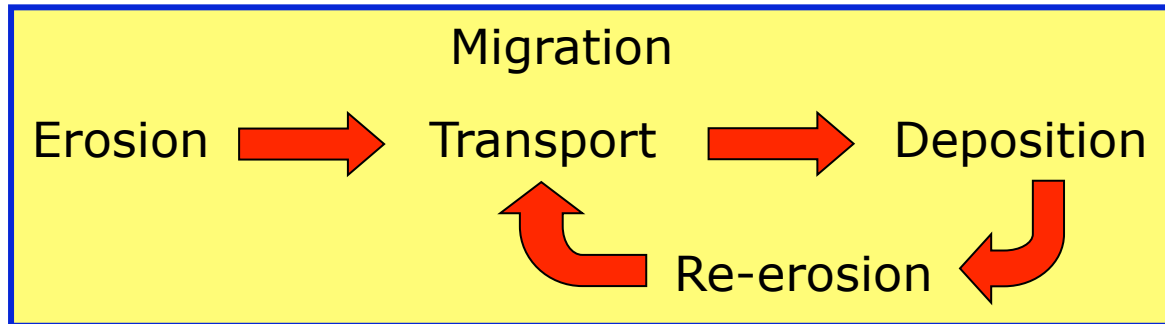
Outline

- 1. *JET carbon sources*
- 2. **JET carbon contamination**
 - **Contamination measured spectroscopically**
 - **Carbon fuelling efficiency determined by methane injection**
 - **Fuelling efficiency determined by carbon ionization closeness to LCFS**
 - **ELM is important but difficult to understand**
- 3. *JET carbon migration*
- 4. *Relate to ITER*

migration

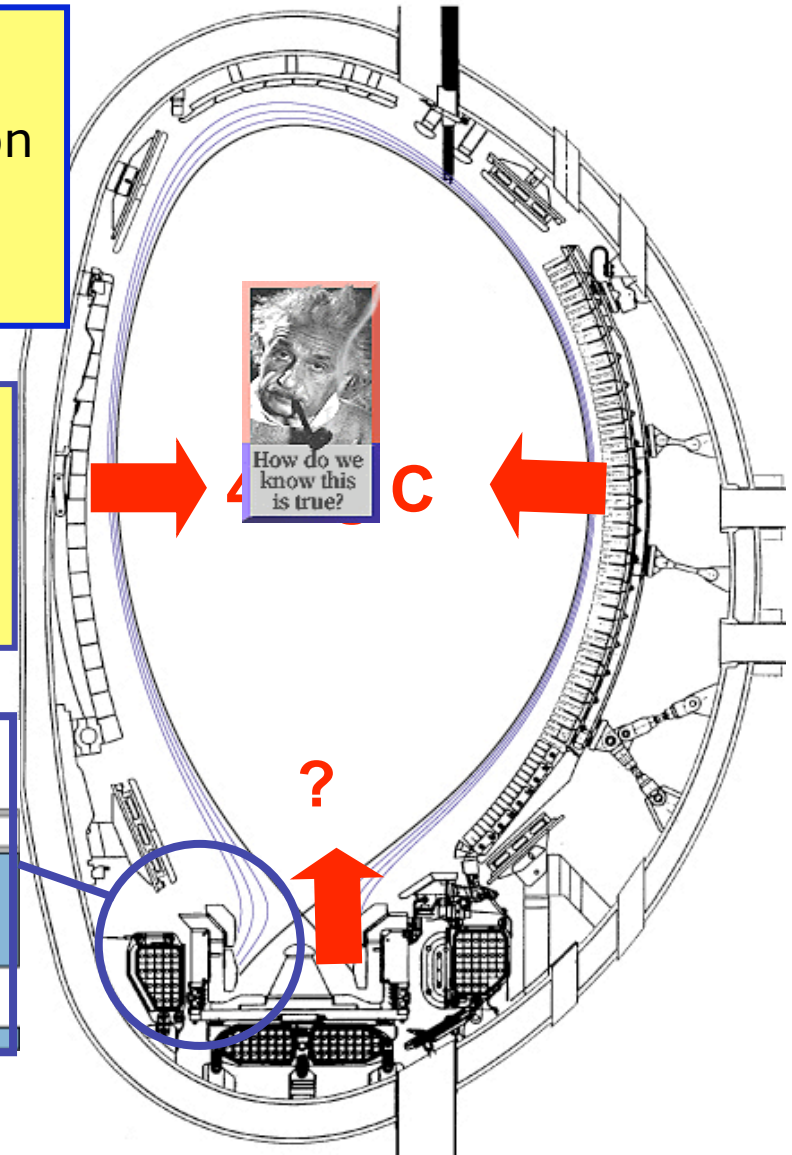
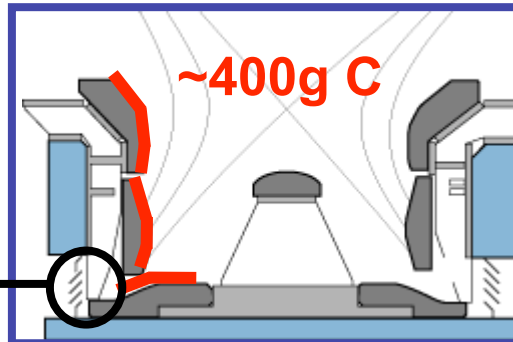
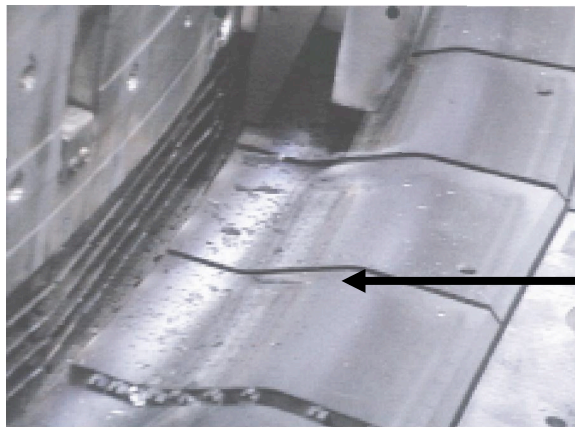
- Impurities contaminate the core but individual impurity ion only spends about a confinement time in the core
- Eventually the impurity travels to some surface, where it can be re-eroded, re-contaminate, etc until it somehow reaches a surface where it is not re-eroded
- The impurity has migrated from its source location to the non-eroding surface.

Global migration accounting for Carbon on JET

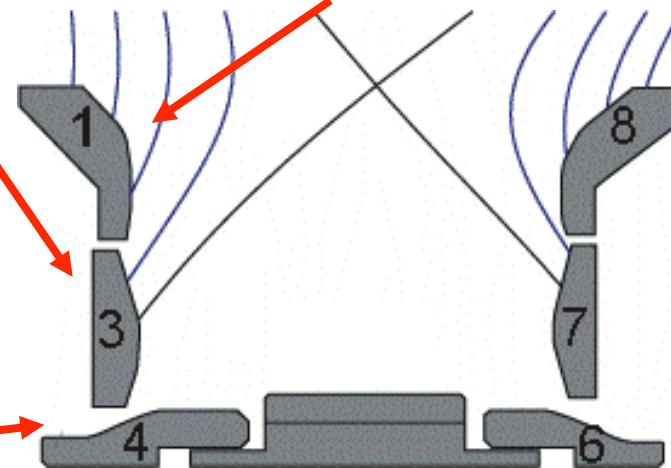
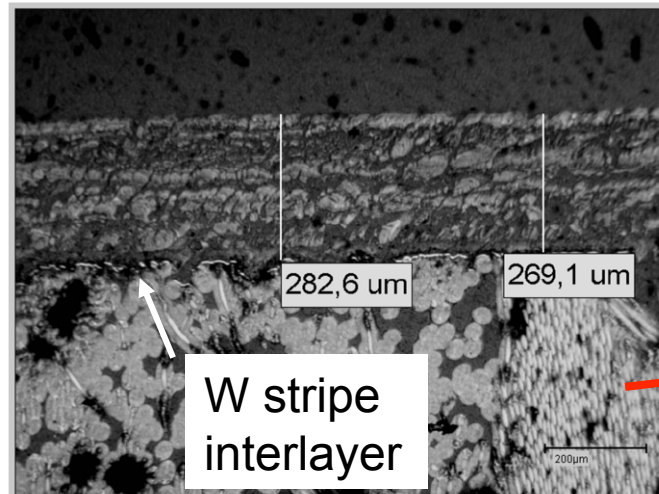
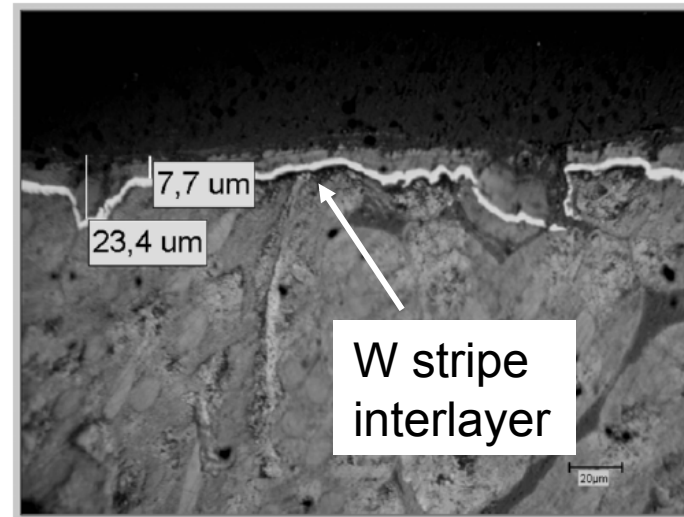
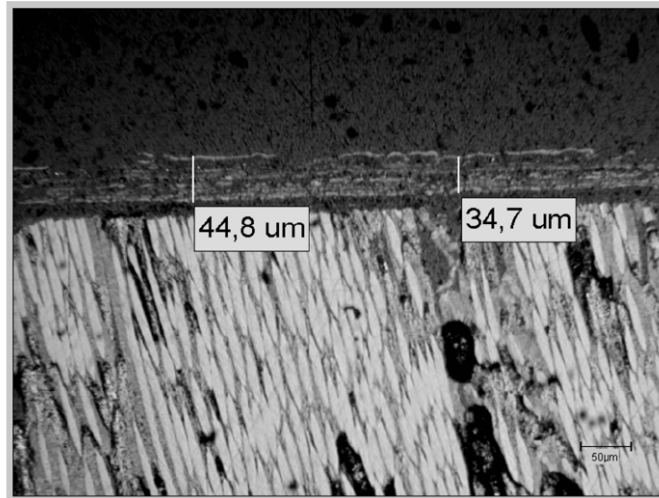


Global balance for period of operation from 1999-2001, 14 hours of plasma

50400 s, 5748 shots on JET ~ **50 shots on ITER**

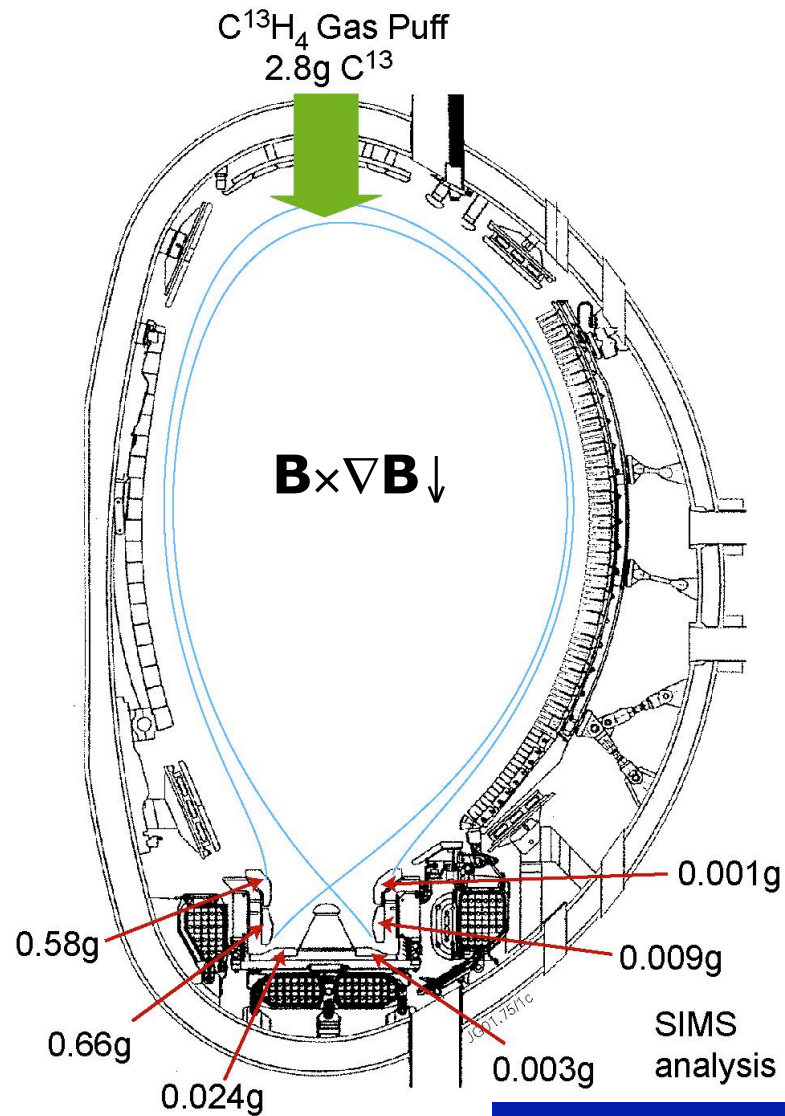


Carbon films accumulate in remote areas



A layer thickness of 100 μm = $6 \cdot 10^{20}$ C/cm²
Extent: 5cm (poloidal) \times 1600cm (toroidal)
Corresponds to: $4.8 \cdot 10^{24}$ C = 100 gC

^{13}C Experiments: inject a marker to locate deposits



$^{13}\text{CH}_4$ injected on last day before vent

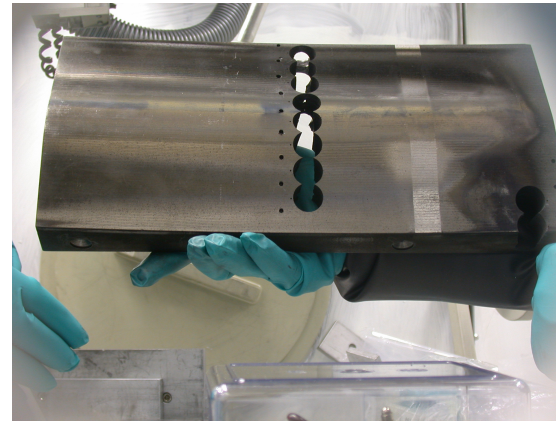
- Identical pulses, specific plasma conditions instead of complex history
- Remove tiles, perform Secondary Ion Mass Spectroscopy (SIMS) analysis

Injection from the top (2001):

- 45% found at inner divertor

Injection from outer divertor (2004):

- 11% found at inner divertor
- 17% found at outer divertor



^{13}C deposition following injection near outer strike point



^{13}C deposition following injection near outer strike point



Also injection from vessel top

^{13}C deposition following injection near outer strike point



Also ^{12}C from campaign

^{13}C deposition following injection near outer strike point



^{13}C deposition following injection near outer strike point



Model for top injection

^{13}C deposition following injection near outer strike point



Model for outer strike
point injection

^{13}C deposition following injection near outer strike point

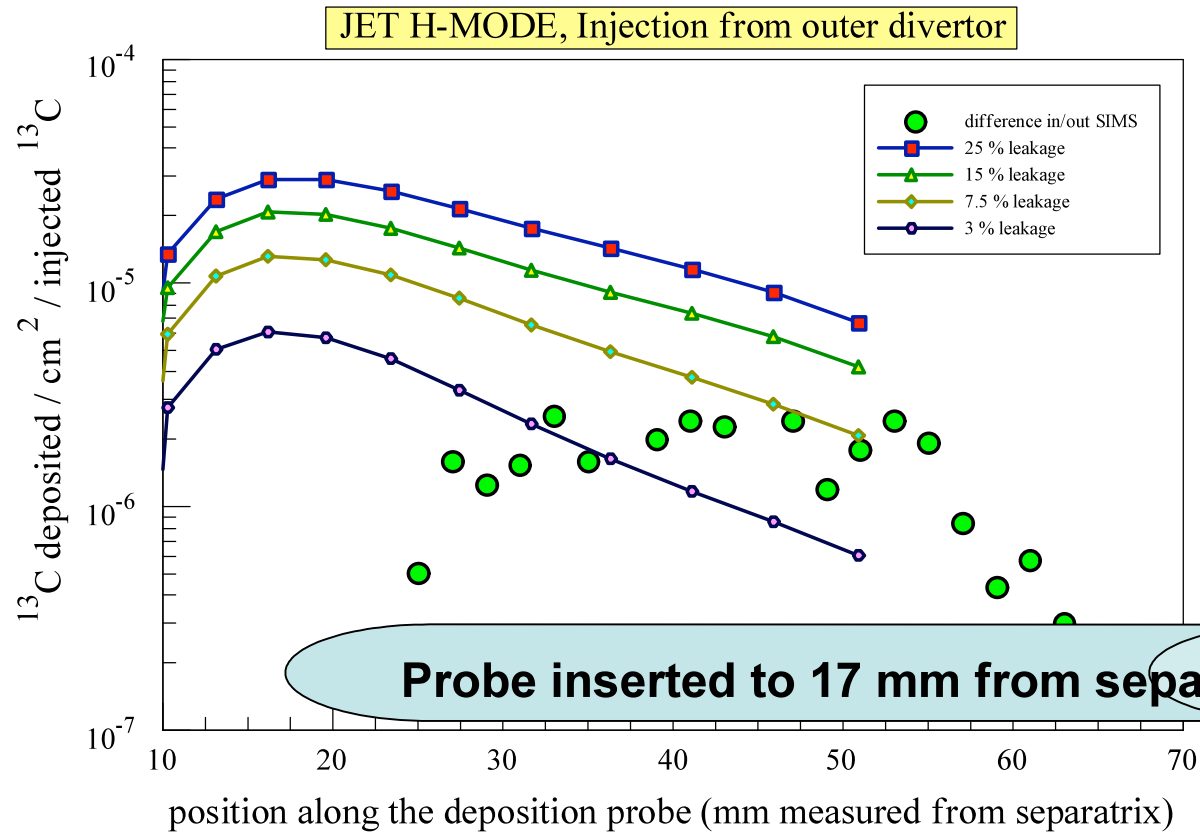


Model including
leakage from outer div

^{13}C deposition following injection near outer strike point



Model including re-erosion



Deposition on the Reciprocating probe at the vessel top indicate 3 times more ^{13}C deposition on the side facing the outer target and in the direction of the SOL flow. The modeling indicates a different spatial variation possibly indicating re-erosion of the deposited ^{13}C .

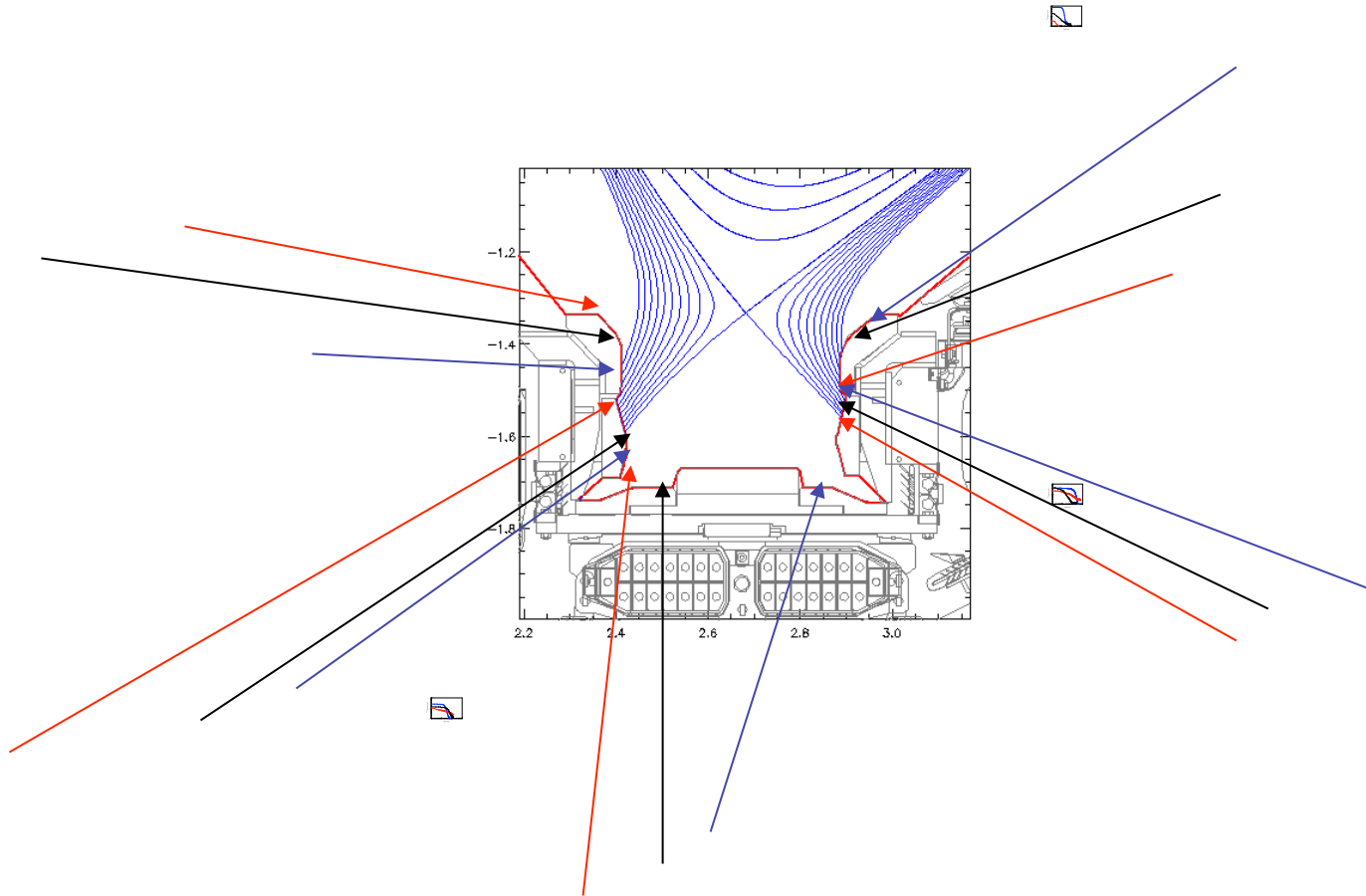






^{13}C set to implant in walls

Depth profiles of ^{13}C with small surface deposit and larger penetration into target, are ones with significant re-erosion



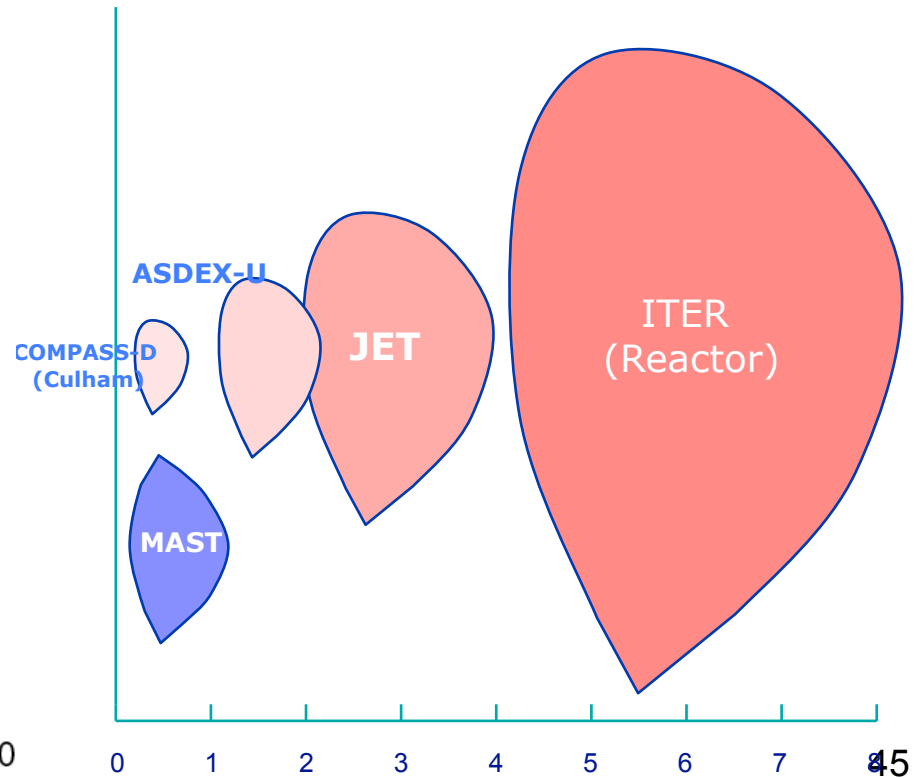
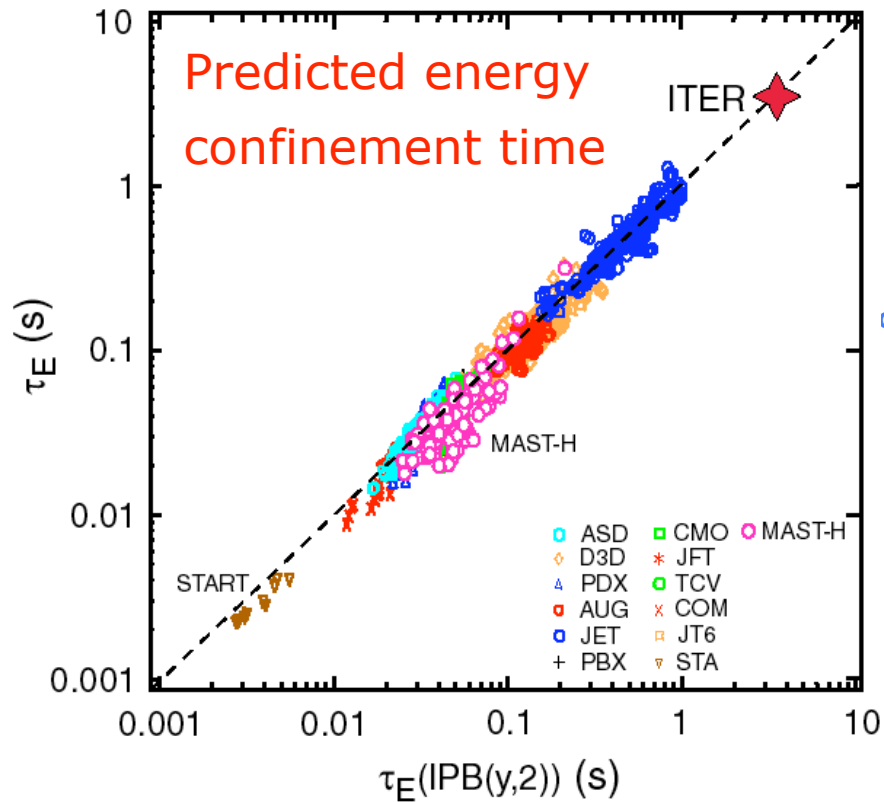
Outline

- 1. *JET carbon sources*
- 2. *JET carbon contamination*
- **3. JET carbon migration**
 - **Migration to remote areas occurs**
 - **^{13}C marker experiments have some characteristics of campaign integrated migration**
 - **Re-erosion is important and occurs where sputtering is high**
 - **Some features of ^{13}C migration can be understood from initial transit physics**
- 4. *Relate to ITER*

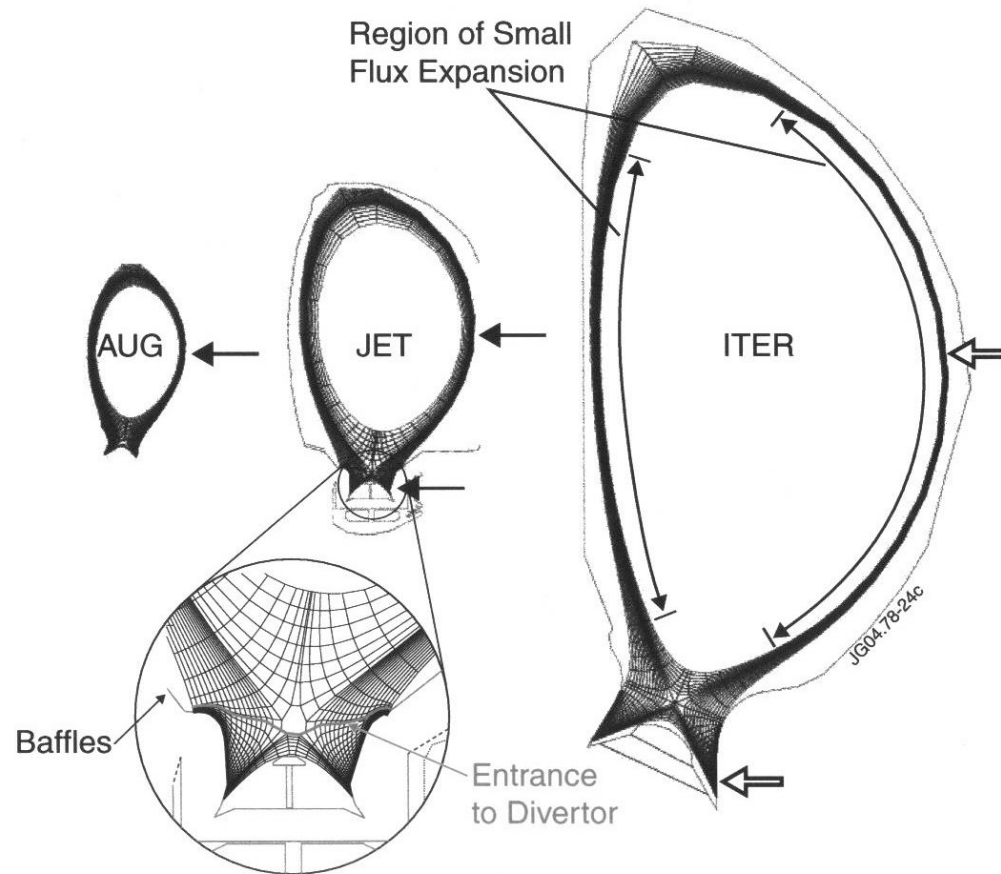
From JET to ITER

Exhaust Power (MW)	30	200	[S]
Materials	C	Be/W	[S]
Surface Area (m²)	150	500	[S]
SOL temperature (eV)	85	150	[S]

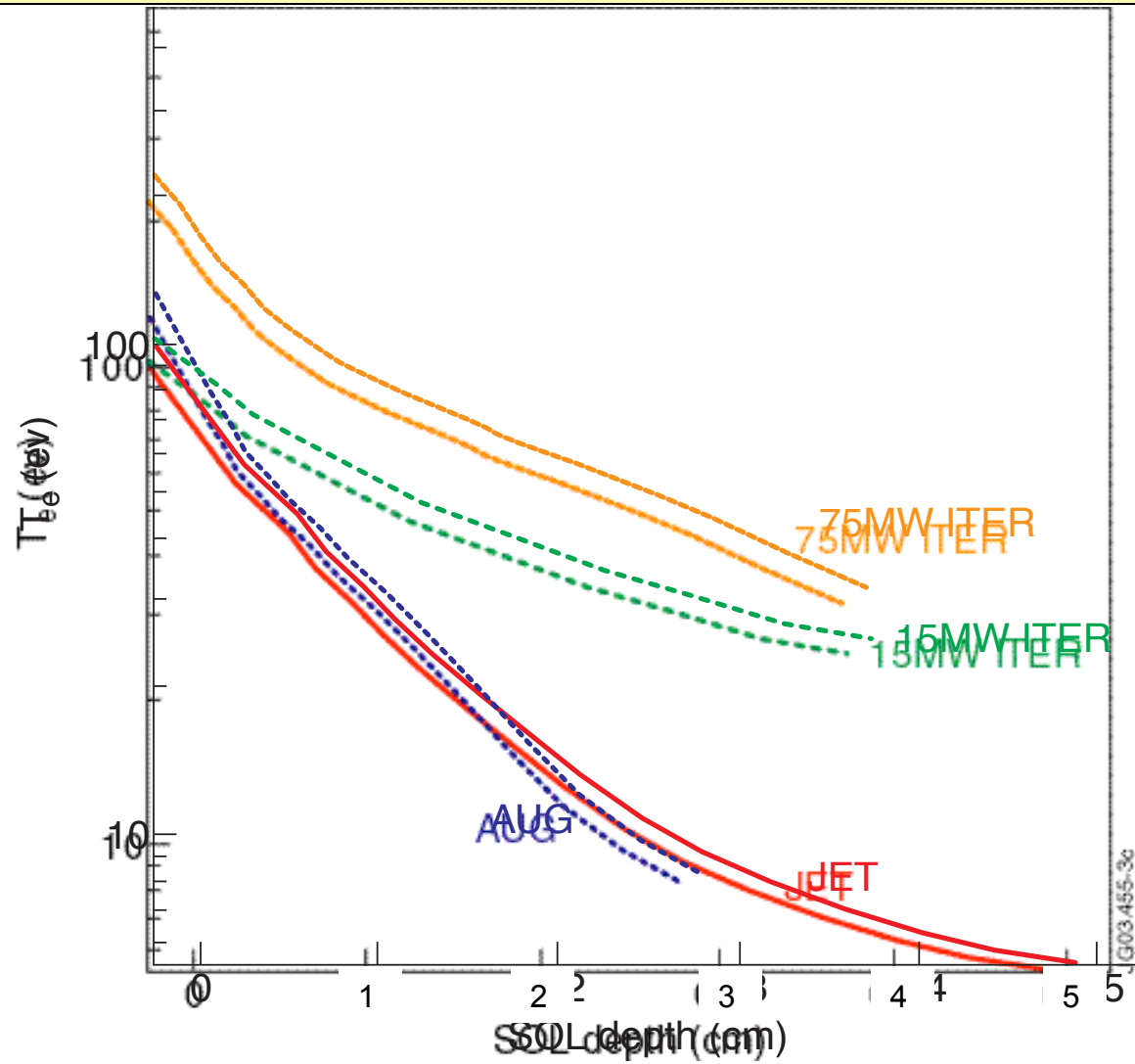
Volume (m³)	100	1000	[C]
Divertor size (m)	0.3	1.25	[C]
Parallel length (m)	80	170	[C]
Duration (sec)	10	1000	[M]



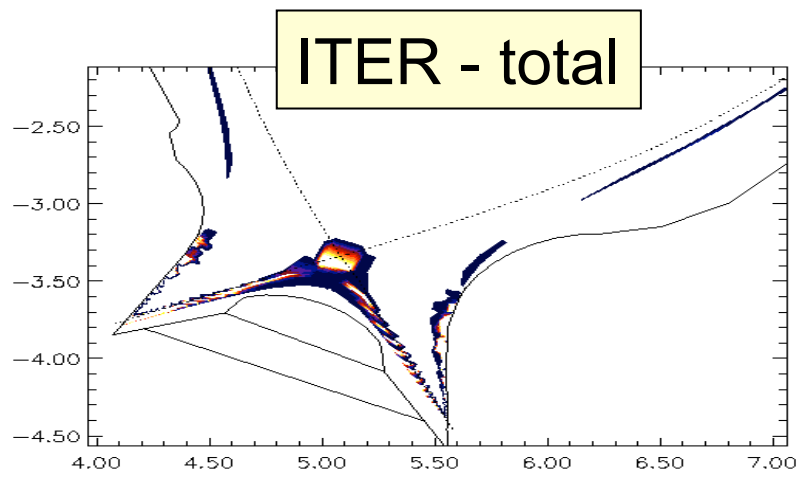
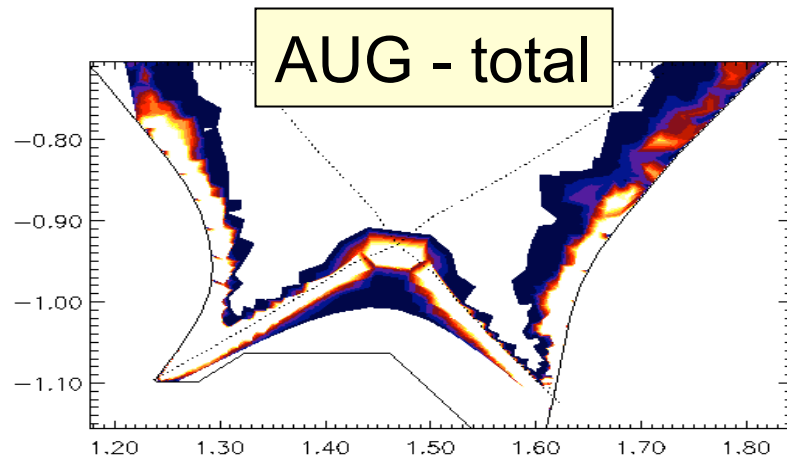
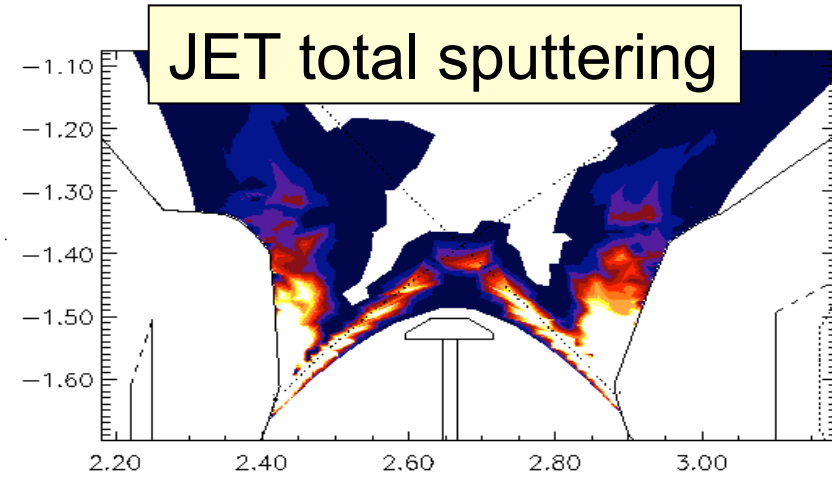
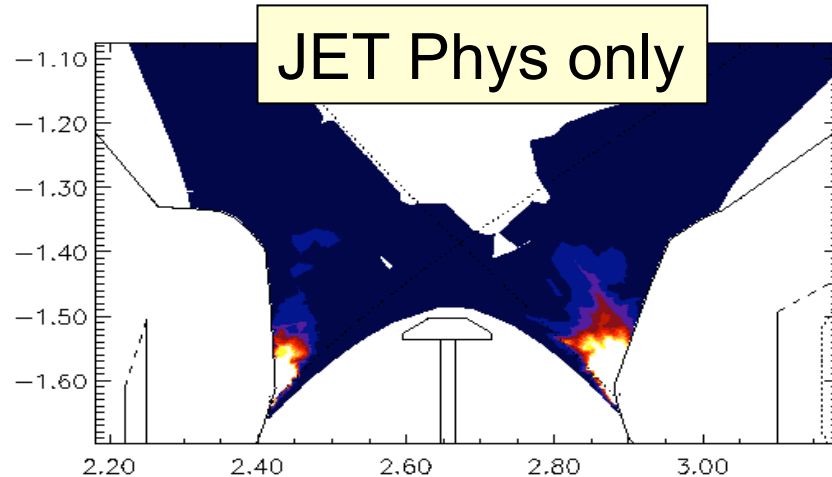
Using the EDGE2D calculations which described the JET erosion, contamination, and migration, can also switch to AUG and ITER grids to understand if the same physics governs those machines



ITER SOL is hotter and narrower than JET, featuring more contact at the vessel top due to the high triangularity of ITER

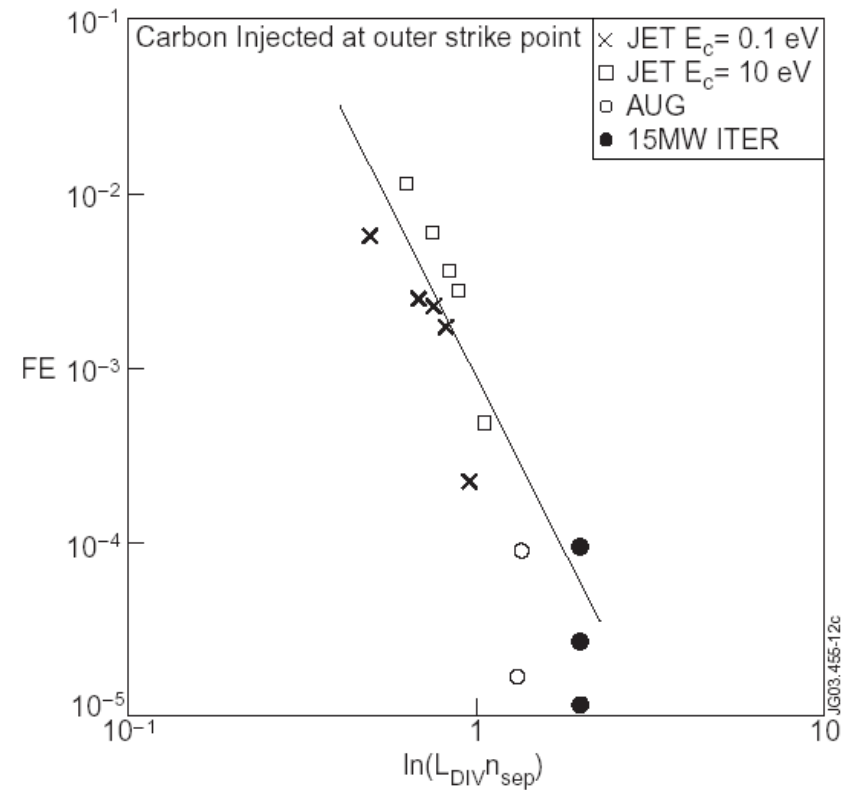
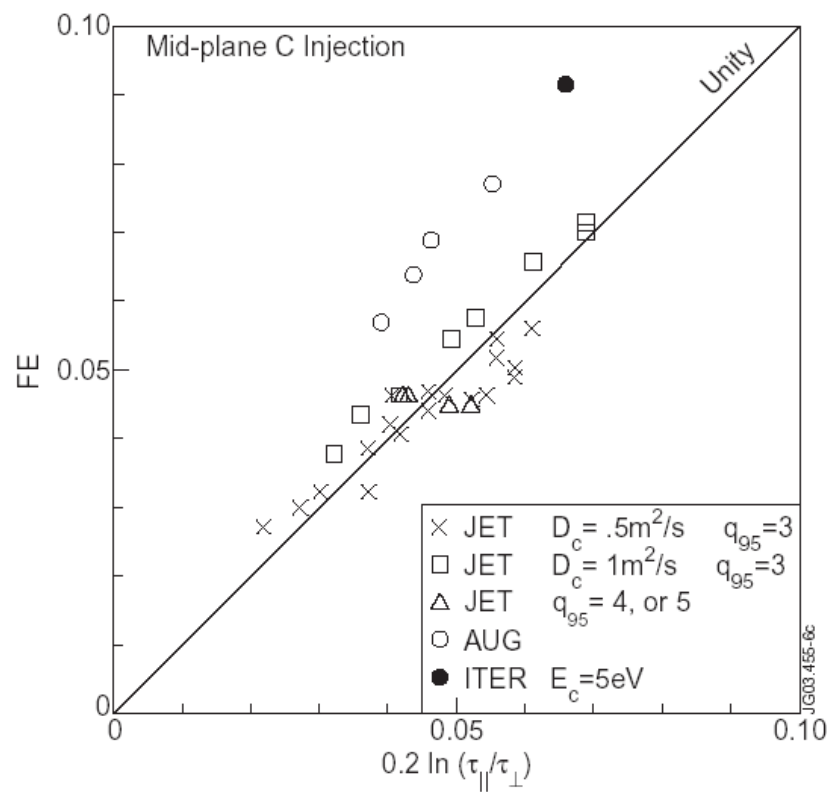


EDGE2D calculated carbon ionization in JET, AUG, and ITER, assuming carbon in each machine. Notice ITER has impurity ionization much further from the main chamber

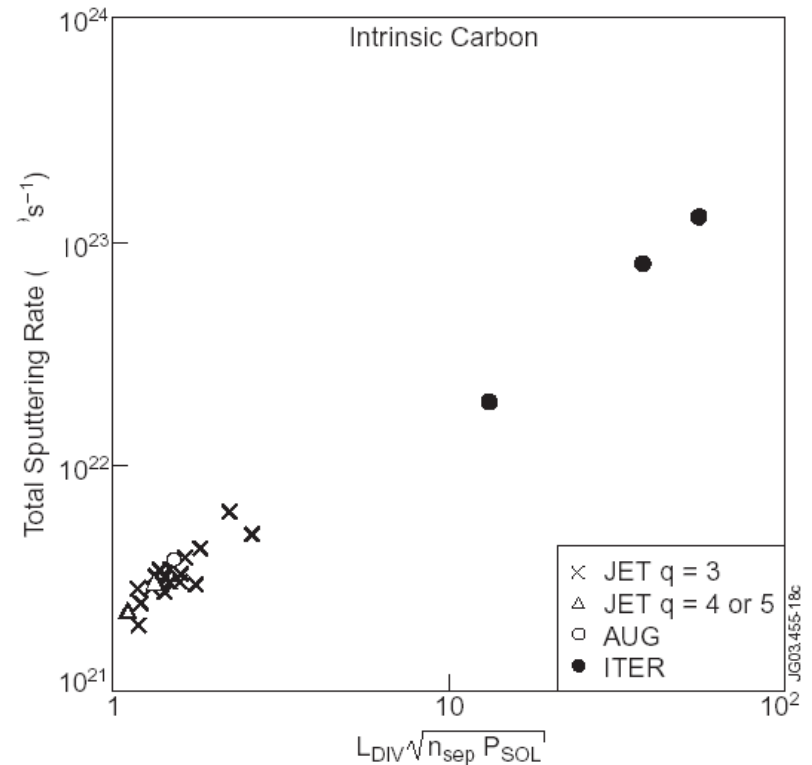
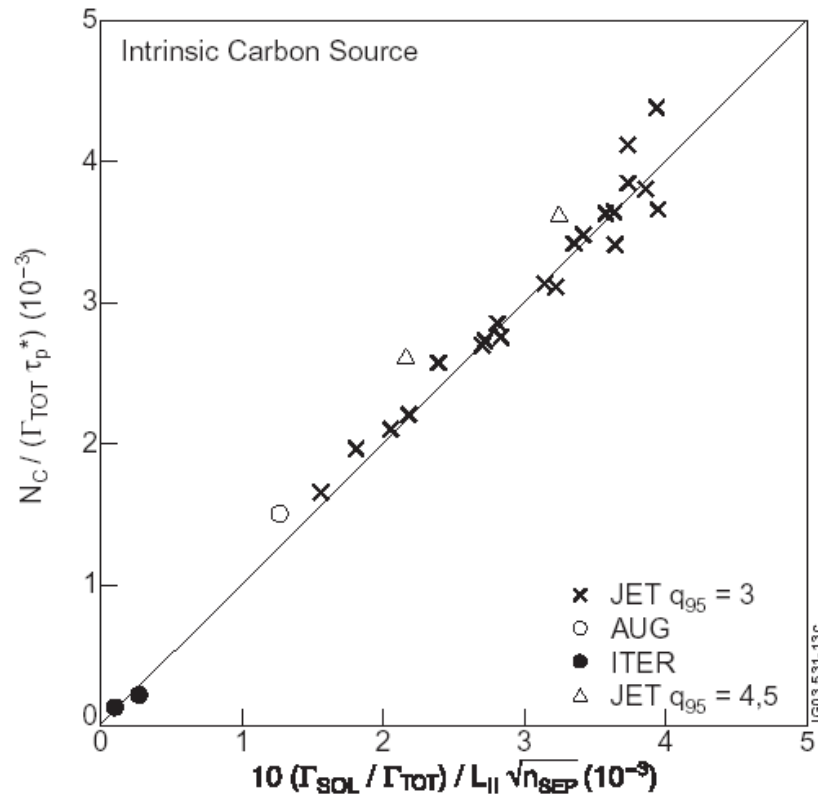


Impurity fuelling efficiency is a poor calculation for ITER, but does indicate that the divertor fuelling efficiency is much lower for ITER than for JET

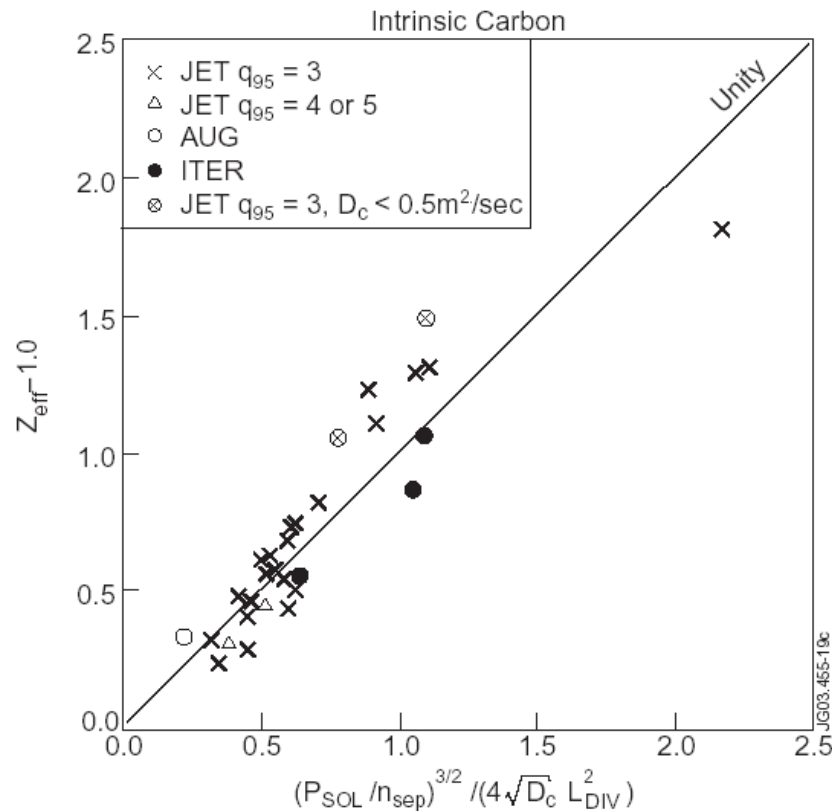
The mid-plane ITER fuelling efficiency is high, but that is due to the 15 MW SOL power and 5 eV C neutrals assumed in order to get the carbon to ionize in the ITER grid



Scaling the mid-plane fuelling efficiency for ITER (somehow) and averaging the fuelling efficiency over the sputtered surfaces indicates that ITER should have 10-15 times better screening coupled with 10-100 times more sputtering, if composed of carbon

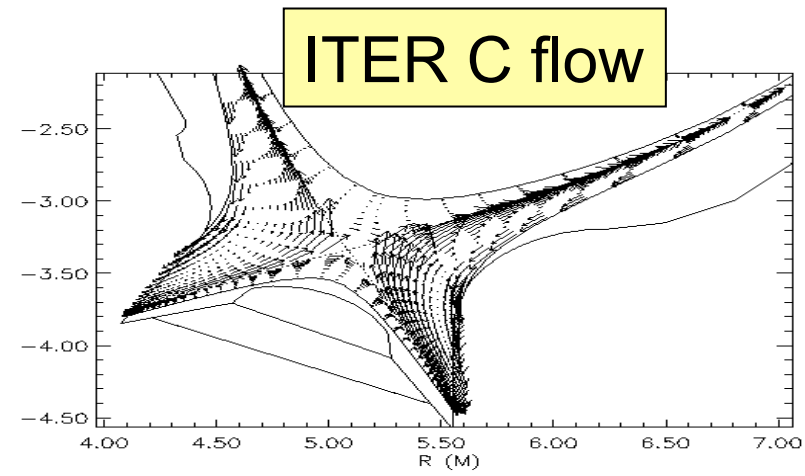
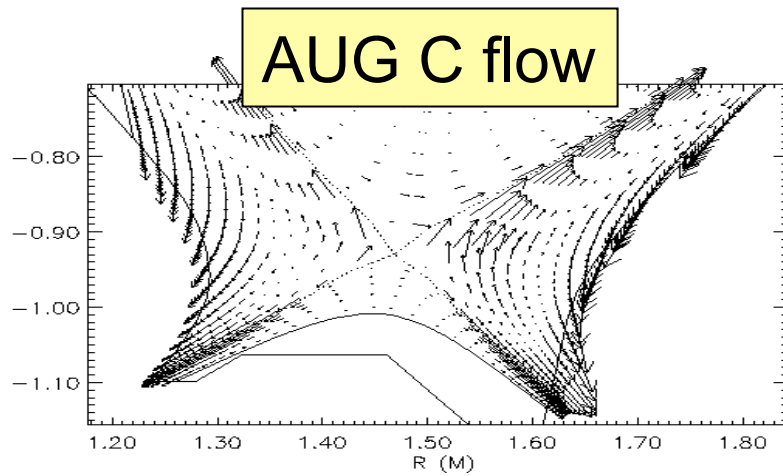
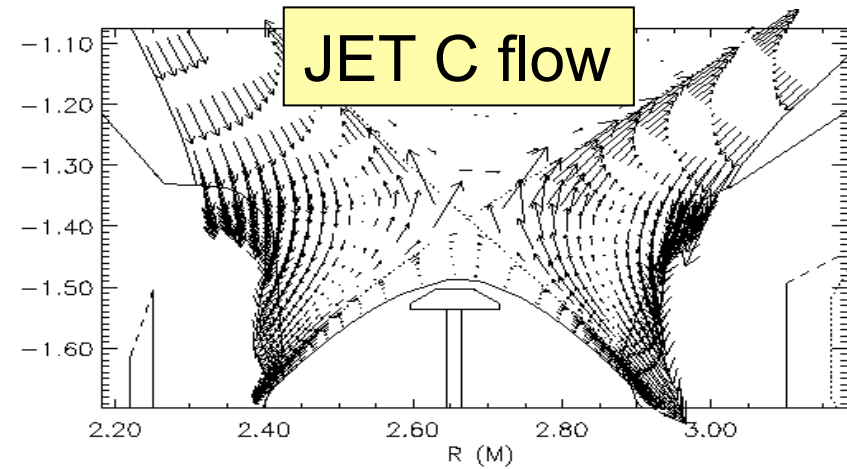
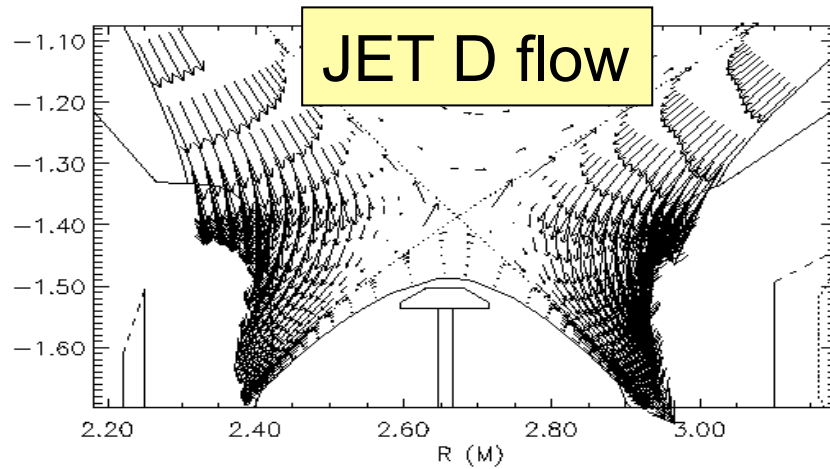


The final impurity content is calculated to be similar to JET, but worse than the AUG plasma studied, assuming ITER were all carbon

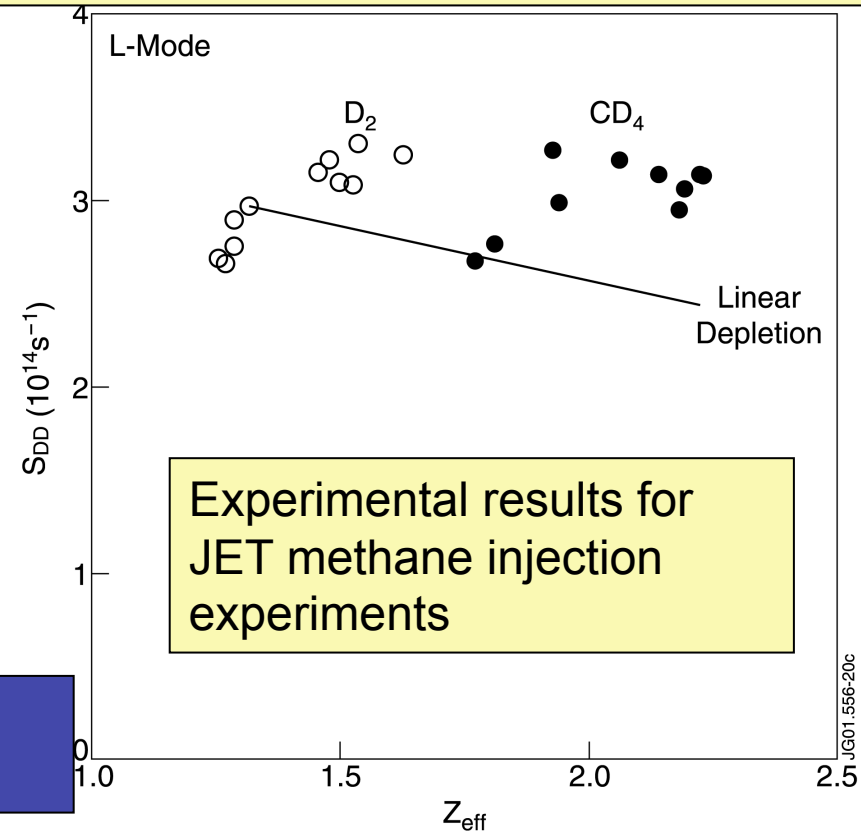
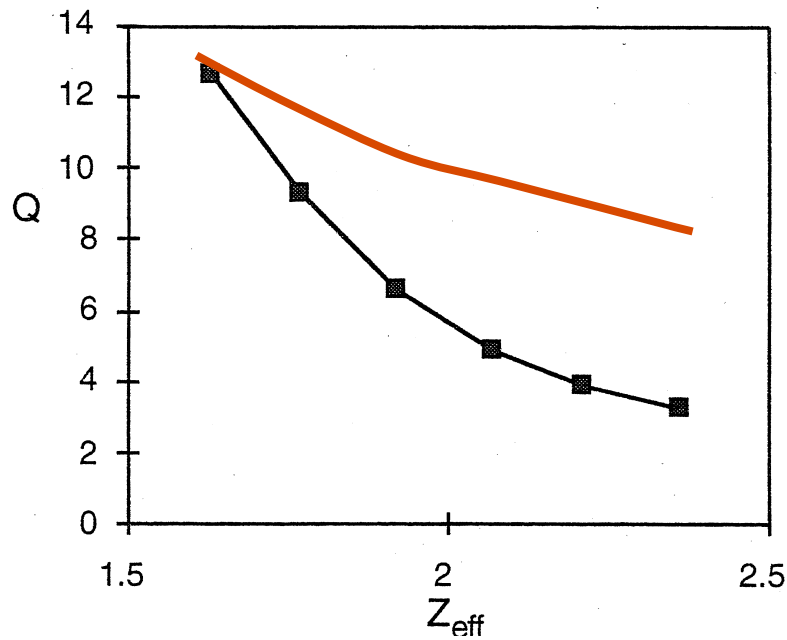


quantity	units	AUG	JET	ITER	ITER
P_{SOL}	MW	2	2.5	15	75
R_X	m	1.4	2.7	5.1	5.1
P_{SOL} / R_X	MW/m	1.3	.9	3	15
L_{\parallel}	m	65	70	170	170
L_{DIV}	m	0.25	0.3	1.25	1.25
T_{sep}	eV	102	85	92	178
n_{sep}	10^{18} m^{-3}	17.3	9.4	7.5	26.3
D_{Bohm}	m^2/s	1.55	1.28	1.37	2.58
Γ_{phys}	$10^{19}/\text{s}$	23.4	63.2	333	1283
Γ_{tot}	$10^{19}/\text{s}$	361	348	1902	$1.3 \cdot 10^4$
Z_{eff}	Physical sputtering	1.06	1.21	1.48	1.13
Z_{eff}	total sputtering	1.33	1.58	1.56	2.06
FE_{DIV}	%	0.0018	0.68	0.0027	0.012
FE_{MP}	%	5.5	4.3	1.8	1.5

Impurity flow patterns for JET, AUG, and ITER indicating similar impurity flow reversal for the 3 machines, ie ion transport from divertor to main chamber SOL



One confusing aspect of impurity contamination (or alpha ash removal) studies is its expression as a fuel depletion problem. Actually, the fusion reaction rate depends only upon the reactant densities, and not upon the densities of other particles such as impurities or electrons. However, since plasma electron density is usually measured in plasmas, this has caused us to pretend that other impurity concentrations would deplete the fuel. In reality, additional impurities will increase the electron density but leave the reaction rate unaltered.



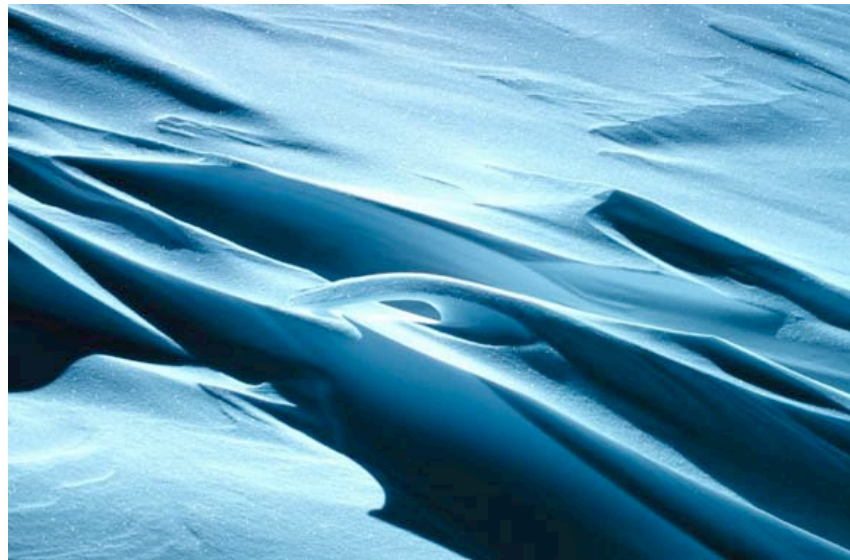
Experimental results for JET methane injection experiments

V. Mukhovatov PPCF 42, A223 (2000)
 $P \propto n_D n_T \langle \sigma v \rangle$ for ITER

JG01.556-20c

Today we model the tokamak deposits starting from the source, its migration to a surface and possible re-erosion.

Instead, with a 100X longer experiment, we will probably ignore the source like we do with snow and sand drifts, and model the ability of the surfaces to shield the deposits.



Snow drifts in Antarctica



Sand dunes in a desert

Deposition in castellated tiles



Tiles from previous JET experiments in 1998

Gaps : 6 - 10 mm
Inventory 30%
compared to surface


Toroidal direction

Sliced to reduce eddy currents
Castellations for stress relief

Grooves:
0.6 mm wide, 10 mm deep,
Inventory 2% compared to
surface

Outline

- *1. JET carbon sources*
- *2. JET carbon contamination*
- *3. JET carbon migration*
- **4. Relate to ITER**
 - **Projections from JET are complex**
 - **Longer duration, higher SOL temperature, plasma contact at the vessel top, different materials, longer scale lengths are all important**
 - **ELMs and ELM mitigation effects on impurities are difficult topics**
 - **Larger sources are offset by better screening**
 - **Expect ITER will be learning as it operates**